Atmospheric Deposition to the Athabasca Oil Sands Region Using Snowpack Measurements and Dated Lake Sediment Cores

1.2
Report Series

Oil Sands Monitoring Program Technical Report Series

Canada

Alberta

Atmospheric Deposition to the Athabasca Oil Sands Region Using Snowpack Measurements and Dated Lake Sediment Cores

Jane Kirk[1], Derek Muir[1], Carlos Manzano[1], Colin Cooke[2], Johan Wiklund[1], Amber Gleason[1], Jamie Summers[3], John Smol[3], Joshua Kurek[4]

[1]Environment and Climate Change Canada

[2]Alberta Environment and Parks
[3]Queen's University
[4]Mount Allison University

This publication can be found at: https://open.alberta.ca/publications/9781460140260

Recommended citation:
Kirk, J., Muir, D., Manzano, C., Cooke, C., Wiklund, J., Gleason, A., Summers, J., Smol, J. & J. Kurek. Atmospheric deposition to the athabasca oil sands region using snowpack measurements and dated lake sediment cores. Oil Sands Monitoring Program Technical Report Series No. 1.2. 43 p.

June 2018
ISBN 978-1-4601-4026-0

Foreword

Since February 2012, the governments of Alberta and Canada have worked in partnership to implement an environmental monitoring program for the oil sands region. In December 2017 both governments renewed their commitment to working together with Indigenous communities in the region by the signing the *Alberta-Canada Memorandum of Understanding (MOU) Respecting Environmental Monitoring in the Oil Sands Region*. The MOU establishes the foundation for an adaptive and inclusive approach to program implementation ensuring that the program is responsive to emerging priorities, information, knowledge, and input from key stakeholders and Indigenous peoples in the region.

The Oil Sands Monitoring Program is designed to enhance the understanding of the state of the environment and cumulate environmental effects as a result of oil sands development in the region though monitoring and publically reporting on the status and trends of air, water, land and biodiversity. Its vision is to integrate Indigenous knowledge and wisdom with western science to design, interpret, assess, report and govern the program.

Canada and Alberta have provided leadership to strengthen program delivery, and ensure that necessary monitoring and scientific activities meet program commitments and objectives. The oil sands industry provides funding support for the program under the Oil Sands Environmental Regulation (Alberta Regulation 226/2013). Key findings and results from the program inform regional resource management decisions and importantly, are considered as an objective source of scientific interpretation of credible environmental data.

A mandated cornerstone of the program is the public reporting of data, status and trends of environmental impacts caused by development of oil sands resources. The Oil Sands Monitoring Program *Technical Report Series* provides an objective, and timely, evaluation and interpretation of monitoring data and information collected across environmental media of the program. This includes reporting and evaluation of emission/release sources, fate, effects and transport of contaminants, landscape disturbance and responses across theme areas including atmospheric, aquatic, biotic, wetlands, and community based monitoring.

Executive Summary

In 2011, the Governments of Canada and Alberta designed a monitoring plan for surface water quality and quantity, air quality and biodiversity of the lower Athabasca River between Fort McMurray and its confluence with Lake Athabasca. The purpose of this report is to answer the following key questions identified in the Joint Oil Sands Monitoring Plan (JOSM) regarding atmospheric deposition of contaminants to the landscapes and water bodies of the Athabasca Oil Sands region:

1. What is the direct aerial deposition of the identified contaminant species to the surface of the Athabasca River and its tributaries?
2. What is the aerial deposition to the landscape in the Athabasca River Basin from Fort McMurray to the Athabasca delta?
3. How does the aerial deposition to the landscape affect water quality in the tributaries and main stem of the Athabasca River?

This study uses snowpack measurements and dated lake sediment cores to investigate deposition of contaminants, which include polycyclic aromatic compounds (PACs) and numerous inorganic and organic contaminants, such as mercury (Hg). Snowpack measurements are used because they are a temporally integrated measure of wet and dry atmospheric deposition spanning the period from first snowfall to sampling. In the absence of pre-development monitoring for this region, we used high resolution, dated lake sediment cores to assess the natural range in contaminant deposition. Examination of zooplankton, chironomid and diatom fossil remains, as well as climate proxies in dated lake sediment cores, allowed us to determine the impacts of changing contaminant deposition on biological communities. Analyzes of snowpack and lake sediment cores collected from 2011-2014 show that deposition of contaminants, including PACs and a variety of metals including mercury and methyl mercury, is most elevated close to major developments and remains above background for 50-75 km from major developments. These findings agree with those from other multi-media measurements including air and precipitation monitoring under JOSM, as well as with lichen measurements carried out by the Wood Buffalo Environmental Association. Results from these same multi-media measurements indicate that fugitive dusts are important contributors to contaminant deposition in the Athabasca Oil Sands region. Analyzes of dated lake sediment cores reveal that atmospheric deposition of PACs and inorganic contaminants has increased since oil sands development began in the 1960s. In addition, lake primary productivity has increased and invertebrate communities have changed over the past ~100 years, likely due to climate-driven changes in the region.

Our results point to several priorities for future monitoring and research, including continued snowpack monitoring to determine short-term temporal trends in contaminant deposition and to quantify post-depositional processing of key contaminants, such as mercury and methyl mercury. Results from the snowpack and lake sediment core program as well as from air and precipitation monitoring suggest that analysis of source materials combined with identification of novel industrial and/or natural sourced markers will support quantification of the relative importance of various industrial and natural processes to contaminant deposition. Finally, results from multi-media analyzes indicate more information on emissions is needed to accurately model atmospheric contaminant transport, transformation and deposition to the oil sands region.

Table of Contents

List of Tables

List of Figures

1. Introduction

Various studies have reported atmospheric deposition of contaminants, including polycyclic aromatic compounds (PACs) and numerous inorganic contaminants, such as mercury (Hg), to the landscapes and water bodies of the Alberta Oil Sands region (Kelly et al. 2009 and 2010, Graney et al. 2012, Kurek et al. 2012, Studabaker et al. 2012, Cho et al. 2014, Kirk et al. 2014). In this introduction, we provide a general introduction to PACs and inorganic contaminants, with a focus on Hg, in the environment, a synopsis of previous research carried out to examine atmospheric deposition of PACs and inorganic contaminants in the oil sands region, and a discussion of monitoring needs.

PACs are one of the most widespread organic pollutants in the environment and are of concern because several congeners are toxic and carcinogenic (US Department of Health and Human Services 1995, Boffetta et al. 1997, Bostrom et al. 2002, Baird et al. 2005). PACs are present in fossil fuels and are formed by incomplete combustion of carbon-containing fuels; thus, they are emitted from industries such as smelters and pulp and paper mills, as well as from natural forest fires, oil seeps, and organic matter degradation (Yunker and MacDonald 1995, Savinov et al. 2000). They consist of two or more aromatic rings and include heterocyclic analogs in which carbon atoms in the structure are replaced by nitrogen or sulphur (Lima et al. 2005).

Three main classes of PACs are resent in the environment: unsubstituted PACs (unPACs), alkylated PACs (aPACs) and heterocyclic PACs (including sulfur containing dibenzothiophenes (DBTs) and nitrogen containing azarenes), with less known about the ecotoxicological effects of the aPACs and heterocyclics. Different types of combustion yield unique combinations of PAC products, which allow sources to be identified by examination of different PAC ratios (Lima et al. 2005). unPACs, aPACs, and DBTs are important constituents of raw bitumen within the Athabasca Oil Sands region (Akre et al. 2004) and thus are potentially emitted from processing activities. Data from the Environment Canada National Pollutants Release Inventory (NPRI) show that PACs emissions from bitumen upgrading facilities within the community of Wood Buffalo are currently ~306 kg/year. Contaminant emission estimates from other potential airborne sources, such as vehicle emissions, volatilization from tailings ponds (Parajulee and Wania 2014), and blowing dusts from open pit mines, exposed coke piles (Zhang et al. 2016), and deforested areas not reported to NPRI by industry.

A large number of inorganic contaminants of concern are found in the environment, and each has potential environmental effects. This report focuses on Hg, a global pollutant that can reach levels of concern in humans, primarily through consumption of fish, seafood, and wildlife (Chen et al. 2012). Methyl mercury (MeHg) is the form of Hg of greatest concern as it is a neurotoxin that bioaccumulates and biomagnifies through food webs; thus, it frequently reaches levels high enough in fishes to result in fish consumption advisories across Canada and the globe. Within the Athabasca Oil Sands region, there are fish consumption advisories for Athabasca River walleye downstream of Fort McMurray (mywildalberta.com). Consumption of local fishes and wildlife is an important aspect of the traditional way of life in this region.

Environmental cycling of Hg is complex, which makes it difficult to determine why organisms are elevated in Hg in one region relative to another. Globally, the largest anthropogenic source of Hg to the environment is through release of gaseous elemental Hg(0) to the atmosphere from industrial activities such as coal fired power plants and metal smelters. Hg(0) can undergo long-range transport, with both local and distant sources contributing to atmospheric deposition of inorganic Hg(II), which is produced by atmospheric oxidation of Hg(0) and is rapidly deposited to landscapes and water bodies (Shroeder and Munthe 1998, Pirrone et al. 2010, Driscoll et al. 2013). Once deposited, Hg(II) undergoes several biogeochemical transformations. One key process is the microbial methylation of Hg(II) to MeHg, which primarily occurs under reducing conditions in lakes and wetlands (Gilmour et al. 1992, Ullrich et al. 2001, Benoit et al. 2003, Driscoll et al. 2013). NPRI estimates that ~52 kg/year of Hg is currently released to the air from the bitumen upgrading facilities; however, it is not currently mandatory for industry to report the form of Hg released or, as with PACs, the magnitude of other airborne emissions. In addition to Hg, 13 metals (Ag, As,

Be, Cd, Cr, Cu, Hg, Ni, Pb, Se, Sb, Tl, Zn) considered priority pollutant elements (PPEs) under the US Environmental Protection Agency's Clean Water Act are also of interest in the oil sands region, as NPRI reports airborne emissions of several of these elements from the upgrading facilities.

Previous studies (Barrie and Kovalick 1980, Kelly et al. 2009, 2010, Cho et al. 2014, Kirk et al. 2014) have used snowpack sampling to examine atmospheric contaminant deposition in the region because the snow pack represents a temporally integrated measure of atmospheric deposition spanning the period from first snowfall to sampling. Unlike most air and precipitation sampling methods, snowpack measurements are also able to capture both wet and dry deposition, which may be particularly important in regions near point sources. In addition, many locations can be sampled and contaminant concentrations can easily be converted to depositional loads if snow water equivalence measurements are obtained. The first snowpack study in the oil sands region was carried out in 1978 (Barrie and Kovalick 1980). Snow was collected at 60 sites within 100 km of the Great Canadian Sands extraction plant, which was then the largest point source in the region. The authors found that snowpack loads of several major ions and cations, and metals Al, V, Mn, V, Fe, and Ni increased with proximity to the extraction plant. They also demonstrated that the snow pack was alkaline near the plant, due to enhanced Ca deposition, but slightly acidic farther away where H^+, sulfate, and nitrate dominated the ion chemistry.

In March 2008, Kelly et al. (2009, 2010) sampled the snow pack at 28 locations along the Athabasca River and its tributaries and found that loadings of total (Σ)PAC (included 42 analytes) and all 13 PPEs, except Se, were elevated within 50 km of site AR6, located central to the major development area and adjacent to the two major bitumen upgrading facilities. In February 2011, Cho et al. (2014) sampled the winter snow pack at 94 locations using a star-shaped design centred around the same industrial region. Elevated ΣPAC deposition associated with bitumen upgraders and mining activities was found within a roughly elliptical shaped area along the north-south transect and near the developments area. While Cho et al. noted that they may have underestimated ΣPAC loadings due to limited sampling near upgraders and mining areas, their winter deposition estimates, based on integration of the exponential decay function (392-979 kg), were in the same range as those of Kelly et al. (550 kg).

Lichens and mosses have been used to examine atmospheric deposition of PACs and metals to the region (Blum et al. 2012, Graney et al. 2012, Studabaker et al. 2012, Shotyk et al. 2014). Lichens have been widely used to examine trends in air pollution because they obtain their nutrients and thus their contaminant loads from deposition of aerosols and gases (Crum 1988, Nash 1989). The major limitation in using lichen and moss for depositional monitoring is that only contaminant concentrations and not depositional loadings can be obtained. Analyzes of tree lichen *H. physodes* sampled from 121 sites within 150 km of the oil sands region in 2008 demonstrated that concentrations of metals Al, V and Pb and PACs (20 analytes at 20 of the 121 were measured for PACs) increased with proximity to major developments (Graney et al. 2012). In contrast, Hg concentrations decreased within 25 km of major developments, which the authors hypothesized was due to a physiological response of the lichen to enhanced SO^2 deposition (Blum et al. 2012). Analyzes of Sphagnum moss collected from 22 ombrotrophic bogs within the same region in 2013 showed a similar spatial pattern in Pb, V, Ni, Mo, Ba, and Th concentrations (Shotyk et al. 2014). The authors emphasized that except for V, which was enhanced in mosses of the region, concentrations of the other metals examined were low relative to those from various locations in the Northern hemisphere. Blais and Donahue (2015) subsequently raised issues with these findings, noting importantly that Shotyk et al. (2014) calculated average concentrations in sphagnum within a distribution that is clearly non-random.

Although the studies described above have demonstrated enhanced contaminant deposition within the major oil sands development area, these post-development studies cannot assess the natural range in variability for the region, which is crucial for development of emissions and loadings targets. In the absence of pre-development monitoring, paleolimnological reconstructions, such as analyzes of contaminants in dated lake sediment cores, allow us to assess the magnitude of post-development shifts in contaminant deposition relative to natural vari-

ation. Examination of cladoceran/zooplankton, chironomid and diatom fossil remains, as well as climate proxies such as VRS (Visible reflectance spectroscopy) chlorophyll *a* in lake sediment cores, allows us to investigate impacts of changing contaminant deposition on biological communities within the context of long-term environmental change in the region. To date, one published study has used dated lake sediment cores from six lakes located within 10-90 km of the major development area to demonstrate significant increases in PACs deposition after oil sands development began in the 1960s (Kurek et al. 2013). This study was part of the larger JOSM study and results are integrated into this report.

The large body of evidence demonstrating enhanced deposition of PACs and inorganic contaminants, including metals such as Hg, to the oil sands region highlights the need for a cohesive and quantitative, long-term atmospheric deposition monitoring program. The JOSM program not only quantifies contaminant loadings, but also examines spatial and temporal trends in PACs and inorganic contaminant deposition and assesses the impacts of this deposition on terrestrial and aquatic ecosystems. A program based on the central questions and objectives herein was implemented in 2011. The program uses snowpack measurements and dated lake sediment cores to determine short- and long-term temporal and spatial trends in contaminant deposition and is designed so that measurements in these findings can be directly linked to atmospheric, water quality, invertebrate, fish and wildlife contaminant measurements.

Questions

1. What is the direct aerial deposition of the identified contaminant species to the surface of the Athabasca River and its tributaries?

2. What is the aerial deposition to the landscape in the Athabasca River Basin from Fort McMurray to the Athabasca delta?

3. How does the aerial deposition to the landscape affect water quality in the tributaries and main stem of the Athabasca River?

Objectives

Three specific program objectives were developed to address these questions:

1. Determine spatial trends in winter-time atmospheric deposition of contaminants, specifically PACs, metals including total mercury (THg) and methyl mercury (MeHg; the toxic and bioaccumulative form of Hg; may be deposited or produced post-deposition via snowpack methylation), and a variety of other inorganic and organic contaminants, including contaminant loadings for a ~20,000 km^2 region surrounding the major oil sands development and loadings to the lower main stem Athabasca River, the Steepbank, Muskeg and Ells rivers, and the Peace Athabasca Delta.

    a. Examine short-term temporal trends in contaminant loadings to the Athabasca Oil Sands region.
    b. Determine background contaminant loadings for this region.
    c. Determine how aerial deposition to the landscape affects water quality in the tributaries and main stem of the Athabasca River.

2. Determine long-term temporal trends (over the last ~100 years) in atmospheric deposition of PACs and metals to lakes of the Athabasca Oil Sands region within the context of climate-induced changes to lake limnology using analyzes of dated lake sediment cores.

    a. Use analysis of algal and invertebrate fossil remains and VRS chlorophyll a, a proxy for lake primary productivity, to examine climate-induced changes to lakes.

3. Provide recommendations for a long-term monitoring program of atmospheric deposition to the Athabasca Oil Sands region.

This report summarizes current work carried out under the JOSM program on atmospher-

ic contaminant deposition. Results on objectives 1a, 1b and 2a will be presented; work to fully address objective 1c and 3 is ongoing. Activities and results for two sub-components are described below: Spatial trends in winter-time atmospheric deposition of contaminants and Long-term (~100 years) trends in atmospheric deposition of contaminants. The Atmospheric Deposition to the Athabasca Oil Sands Region Using Snowpack Measurements and Dated Lake Sediment Cores program is designed to facilitate integrated assessment of the importance of atmospheric deposition and environmental health. Sampling therefore focused on sites collocated with other oil sands monitoring activities (e.g., amphibians, birds, water quality, etc.).

2. Spatial Trends in Winter-time Atmospheric Deposition of Contaminants

This sub-component uses snowpack measurements to determine spatial trends in winter-time atmospheric deposition of contaminants to the Athabasca Oil Sands region for a ~20,000 km^2 region surrounding the major oil sands development, including the lower main stem Athabasca River, the Steepbank, Muskeg and Ells rivers, and the Peace Athabasca Delta. The contaminants investigated are PACs, metals including THg and MeHg, and a variety of other inorganic and organic contaminants. To quantify net spring-time contaminant loadings to this region, both contaminant concentrations and snow water equivalence were measured at 30-130 sites located at varying distances from the major developments during the period of maximum snowpack depth in spring 2011-2015.

To assess short-term temporal trends in contaminant deposition to this region, snowpack contaminant loadings from ~30 sites were compared to 2008 measurements made by Kelly et al. (2009, 2010) at the same locations. To determine background contaminant loadings for this region, which is particularly important for contaminants that have both local and regional and/or natural and anthropogenic sources, such as Hg, numerous sites located 100-200 km from the major developments were sampled each year, including 10-12 sites in the Peace Athabasca Delta. Currently, snowpack and river water contaminant concentrations and loadings data are being integrated to determine how aerial deposition to the landscape affects water quality in the tributaries and main stem.

2.1 Methods

Study design

To determine spatial trends in winter-time atmospheric deposition of contaminants, complete snowpack profiles were collected at 90-130 sites located varying distances from the major developments each winter. Based on historical snow accumulation data for the Fort McMurray region (Environment Canada) all samples were collected between late February and early March and within six days to ensure maximum snowpack depth and minimize snow alterations over the course of sampling. To determine short-term temporal trends in contaminant deposition to the Athabasca River and tributaries, the 30 sites from Kelly et al. (2009, 2010), including sites located 0-231 km from the major development area on the Athabasca River and six tributaries (Steepbank, Muskeg, Firebag, Beaver, Tar, and Ells rivers) (Kelly et al. 2009, 2010) were sampled from 2011 to 2015. From 2012-2015, the program was expanded to provide sufficient spatial coverage on the landscape to interpolate measured contaminants loads using kriging to produce depositional maps. In 2012, the study was expanded to 89 sites and included 53 sites located along 8 transects moving away from the major development area, and nine sites in the PAD, located ~200 km north of the major developments (Fig. 1). In 2013, in addition to the Kelly et al. sites and the sampling in the PAD, the sampling design was focused on providing support for other aspects of the JOSM program. Sampling was focused on sites where contaminant measurements in air, rain, river water, amphibians, and birds were also being carried out. In 2014 and 2015, the study was again expanded to improve the fit of the kriged depositional maps and capture background contaminant loads for this region more thoroughly. Samples were collected along a gridwork pattern and included sites located >100 km from the major developments in all directions. Samples collected from March 2015 are still being analyzed; thus, data from 2012-2014 will be presented here. PACs data for 2011-2014 will be compared to snowpack data from 2008 from Kelly et al. to determine temporal trends. Data from 2012-2014 will be compared to available snowpack data from 1978 (Barrie and Kovalick 1980).

Sampling sites were accessed by helicopter or snowmobile, and snow samples were collected at 50-100 m upwind of landing sites. Teflon and stainless steel tools used for the snow collections were acid-washed prior to use in the field. Snow pits were dug to the bottom of the snow pack using a stainless steel shovel and a standard two-person "clean hands, dirty hands" protocol to minimize potential contamination as in Kirk et al. (2014) and Kelly et al. (2009, 2010). In 2011 and 2012, a complete snowpack profile at each site was collected using a stainless steel trowel. In 2011-2012, snow cores were also collected for determining snow water equivalence

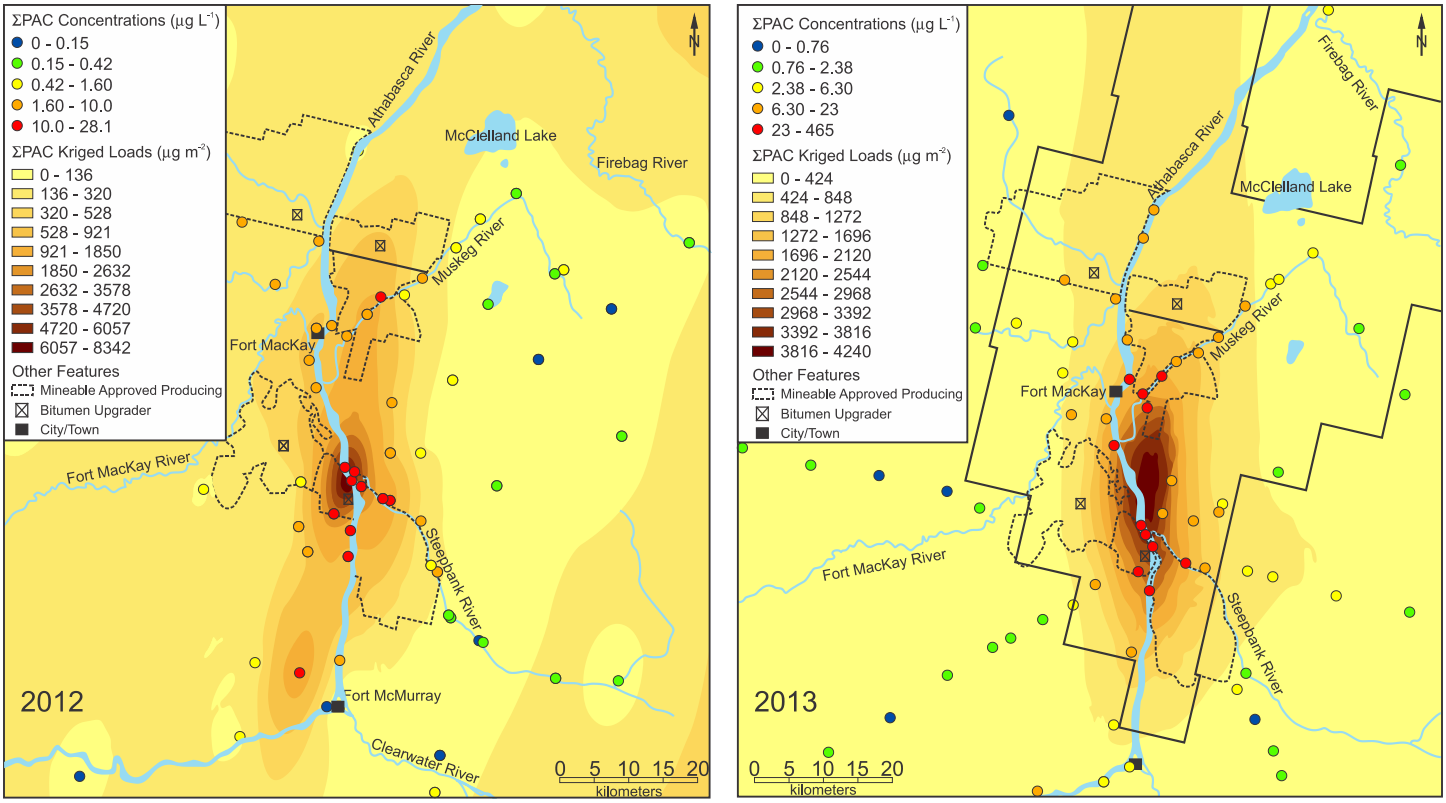

Figure 1. Deposition of ∑PACs to the Athabasca Oil Sands region in winters 2012 and 2013. Interpolated ∑PACs loads ($\mu g/m^2$) produced using ArcGIS Geostatistical Analyst software are overlain by measured concentrations ($\mu g/L$) at each site.

(SWE) using an Adirondack corer. In 2013-2015, custom-made stainless steel corers and stainless steel spatulas were used for collection of snow for both contaminants analyzes and determination of SWE. In all years of sampling, two 13 L pre-cleaned high density polypropylene pails of snow were collected at each site, one for PAC analysis and one for multi-elements and water chemistry analysis. Snow for Hg analyzes was collected into 3 1 L IChem© glass jars (one for THg analysis, one for MeHg, and one that was later filtered and split into samples for THg and MeHg analysis). Each year, the weight and depth of 10 cores were recorded at each site for further determination of SWE. After collection, snow was kept frozen until processing at the Canada Centre for Inland Waters (CCIW), in Burlington, Ontario, Canada.

Sample Analyzes

PACs in snow: Snow buckets were thawed for 2-3 days and processed in a clean room (high-efficiency particulate air (HEPA) and carbon filtered air) at CCIW. Melted snow was filtered through a GF/F filter with 0.7 µm pore size, and passed through a Teflon column packed with 50 g of pre-cleaned XAD-2 resin in series. Filters were extracted with a 1:1 hexane-acetone mixture followed by 100% dichloromethane (DCM) using accelerated solvent extraction (ASE) after being packed in a 33-mL extraction cell between two layers of 2.5 g of Hydromatrix (diatomaceous earth sorbent) and after the addition of 300 ml of surrogate solution. Naphthalene-d8 (61.2%), Acenaphthylene-d8 (68.4%), Acenaphthene-d10 (75.1%), Fluorene-d10 (77.6%), Phenanthrene-d10 (83.2%), Anthracene-d10 (82.7%), Pyrene-d10 (93.7%), Benz[*a*]anthracene-d12 (104.2%), Triphenylene-d12 (93.9%), Chrysene-d12 (90.1%), Benzo[*b*]fluoranthene-d12 (101.1%), Benzo[*e*]pyrene-d12 (100.2%), Bezno[*a*]pyrene-d12 (94.9%), Perylene-d12 (84.6%), Indeno[*1,2,3-c,d*]pyrene-d12 (102.3%), Dibenzo[*a,h*]anthracene-d14 (103.4%), Benzo[*g,h,i*]perylene-d12 (105.0%) and Dibenzothiophene-d8 (32.2%). XAD resin was transferred to an elution column and extracted with acetone followed by DCM, after addition of 300 ml of the same surrogate solution.

Particulate and dissolved fractions were then combined. Briefly, the DCM eluent and ASE

extract were back-extracted using a 3 % sodium chloride solution and dried using sodium sulphate. The concentrated extracts were sent for analysis at the Air Quality Research Division (AQRD) laboratory in Ottawa, Ontario, where they were fractionated using silica gel solid phase extraction (SPE) with hexane and benzene. The benzene fraction was then analyzed by GC-MS, following AQRD protocol 3.03/5.1/M,24 targeting 52 PACs, 25 unPACs, 22 aPACs and 5 DBTs. Field blanks were below 20 % of the most abundant PACs at all sites, except for the more volatile congeners (i.e., C0-C4 naphthalenes, acenaphthene) that showed average values >50%, particularly in 2012. Relative standard deviation (RSD) for individual PACs in all duplicate and triplicate samples averaged 39±25 %, with DBTs having the largest variability. Surrogate recoveries averaged 85±16 %, with d8-DBT being the lowest. Further analytical details can be found in Manzano et al. (2016).

Inorganic and additional organic contaminants in snow: As with PACs samples, snow was melted at room temperature prior to processing. Standard water chemistry analysis and 45 multi-element scans were carried out at the National Laboratory for Environmental Testing (NLET) in Burlington, Ontario. Water chemistry parameters included concentrations of total suspended solids (TSS), total phosphorus (TP), dissolved organic carbon (DOC), particulate organic carbon (POC), and sulphate as well as alkalinity, conductivity, and pH. The 45 elements were analyzed by Environmental Protection Agency (EPA) method 200.8 using an inductively coupled plasma-mass spectrometry (ICP-MS) (EPA 1994) and included numerous crustal and rare earth elements as well as the 13 metals considered priority pollutants elements (PPEs) under the EPA's Clean Water Act. NLET is a certified member of the Canadian Association for Environmental Analytical Laboratories (CAEAL) and undergoes regular external reviews to maintain this accreditation.

Samples for analysis of dissolved THg and MeHg concentrations were filtered through 0.45 µm pore-size nitrocellulose membranes in acid washed Nalgene filter units. All Hg samples were then preserved with concentrated trace metal grade HCl equal to 0.2 % of the sample volume. THg and MeHg concentrations were determined using standard protocols (Bloom et al. 1983, Bloom 1989, Horvat et al. 1993) at the CCIW Low-Level Analytical Laboratory.

Data analysis

Snow water equivalence (SWE) and net loadings were determined for each site as in (Kirk et al. 2006, Kelly et al. 2009, 2010, Kirk et al. 2014).

Briefly, SWE was determined as follows:

$$\text{SWE (kg/m}^2\text{)} = \text{core weight (kg)}/(\pi(\text{corer radius (m)})^2) \quad (1)$$

Average areal water volumes (L/m^2) were then calculated for each site using the formula:

$$\text{Aerial water volume (L/m}^2\text{)} = \text{SWE (kg/m}^2\text{)}/\text{density water (kg/m}^3\text{) X 103 L/m}^3 \quad (2)$$

then multiplied by average concentrations (mg/L) of metals in snow melt to determine springtime loadings of metals (mg/m^2) for each site.

Measured snowpack metals loadings were interpolated for ~20, 000 km^2 area (56.9997, -110.6657 to 57.0032, -112.4782 and 56.4624, -111.451 to 57.7799, -111.3619) using ArcGIS10© Geostatistical Analyst software (Esri, Redlands, California). All kriging surfaces used a simple prediction and log normal, gamma, empirical, or log empirical base distribution depending on the distribution that best fit the data values. The number of neighbours included in each kriging was based on how closely related neighbouring data points were to each other and ranged from 4-8. To test if kriged interpolations significantly over- or under- estimated contaminant deposition, mean measured loadings were compared to kriged means within each kriged area using paired t-tests. No significant differences were found ($p>0.05$), demonstrating that overall, the kriging parameters used resulted in an appropriate fit of measured deposition.

2.2 Results and Discussion

PACs: Spring-time snow pack total (∑)PAC concentrations ranged from 0.03-518 µg/L with highest values found within 2 km of the major developments. To determine the quantity of PACs that enters ecosystems at spring snow melt, springtime snowpack PACs loadings

(μg/m^2) were calculated using snowpack PACs concentrations (μg/L) and average snow water equivalence (L/m^2). ∑PACs loadings ranged from 2.2-to 26,000 μg/m^2, with highest values also found near the major developments. PAC deposition was evaluated following Kelly et al. (2009), where loadings were compared with distance from the major developments (site AR6). ∑PACs loadings were found to decline exponentially with distance from the main developments in 2011 to 2013 (Fig. 2).

Although it is difficult to estimate loadings not affected by oil sands development in the absence of long-term monitoring data, PACs deposition at our most distant sites in the PAD, located ~150-200 km north of the major developments and has no major PACs point sources, averaged only 25±16 μg/m^2 and 13±11 μg/m^2, in 2012 and 2013, respectively (n=9). The ∑PACs concentrations and loadings measured in the PAD were also in the same range as those reported for remote sites in U.S. National Parks (Landers et al. 2010) and in the Tyrolean Alps in Austria (Arellano et al. 2014), which suggests that the PAD sites can be good indicators of background conditions in the oil sands region. The proportion of PACs bound to particles was greater at sites closer to the main developments, and has been attributed to PACs being bound to particles emitted by upgrading facilities and generated during mining activities and land disturbances, and thus depositing close to local sources (Kelly et al. 2009).

∑PACs in snow packs were dominated by aPACs, which did not show a significant change in contribution with distance from AR6, suggesting the presence of other potential sources for aPACs at more distant sites. DBTs, which are known markers for fossil fuel combustion and potentially local open pit mining dust, declined in relative contribution with distance from the major developments. The opposite was observed for unPACs, which are produced by pyrogenic and natural processes, and whose contribution increased with distance from the main developments. The distribution of individual PACs within 50 km of the main developments was dominated by fluoranthenes, phenanthrenes, benzo[*a*] anthracenes and DBTs, with individual contributions ranging from 2 to 8 %. Distribution shifted to more volatile congeners such as naphthalenes at more distant sites, suggesting the presence of different PAC sources. Using Alberta Energy Resource Conservation Board reports to classify sites, the difference in PAC distribution for sites located within ~5 km of upgrading facilities (n=15) and sites located within boundaries of mining (n=23) and in-situ operations (n=4) was evaluated also. The individual contributions of C1-benzo[*a*]anthracenes and C4-DBT were statistically different ($p<0.05$) between samples close to upgraders and samples located close to mining operations. PAC diagnostic ratios were also used as indicators of combustion sources, which suggested a change from petrogenic sources, close to the upgraders, to pyrogenic sources at distant sites. Other diagnostic ratios suggested that particles containing PACs were generated locally, probably during upgrading and mining processes.

Sampling frequency in 2012 and 2013 allowed kriging interpolation to map the spatial patterns in PAC deposition. The kriging interpolation was performed using ArcGIS geostatistical software (Esri, Redlands, CA), and following previous published work (Kirk et al. 2014). A non-uniform deposition pattern of PACs was observed, with areas of maximum deposition located over the Athabasca River between the Muskeg and Steepbank rivers (Fig. 1). Overall, the PAC deposition observed was consistent with recent studies showing higher deposition to the north and south of the major development area (Cho et al. 2014), and with Hg, metals and total suspended solids in the area (Kirk et al. 2014). Kriging interpolation was also used to evaluate ∑PAC deposition to the landscape, as the interpolations incorporate the high variance and non-uniform deposition pattern in PACs deposition. Due to a high sampling frequency, the kriging method is potentially more accurate for the estimation of mass deposition, compared to the integration approach used in previous studies (Kelly 2009, Cho 2014). The ∑PAC mass deposition within 50 km of the main developments was estimated to be 3,690 kg (2012) and 2,000 kg (2013), with contributions of 66 % (2012) and 52 % (2013) of aPACs, and 24 % (2012) and 39 % (2013) of DBTs (Table 1). It was estimated that 500 km^2, equivalent to the area within a 12-km radius, received PACs at rates over 800 μg/m^2 and 500 μg/m^2 during winters 2012 and 2013, respectively. PAC deposition rates were 4-6 times higher within 5 km of the major developments with loads >3,000 μg/m^2 observed for winters 2012 and 2013.

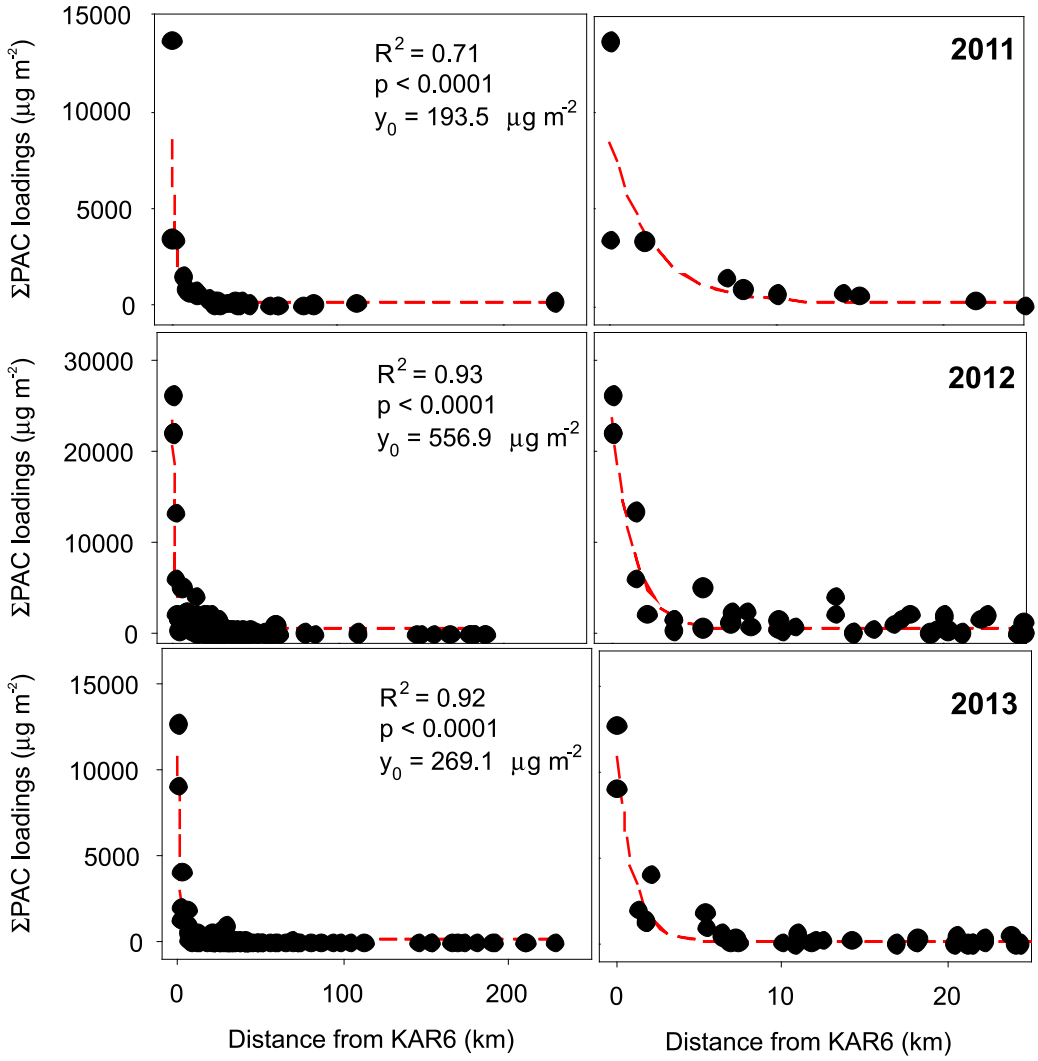

Figure 2. Winter 2011, 2012, and 2013 snowpack ∑PACs loadings versus distance from site AR6, located roughly in the centre of the major oil sands industrial area.

Table 1: PAC deposition estimates for a 4-month period for winters 2008, 2011, 2012 and 2013, within 50 km of main developments.

PACs	2012 Kriging Estimates	Relative Contribution	2013 Kriging Estimates	Relative Contribution
	kg	%	Kg	%
unPACs	369	10	182	9
aPACs	2,439	66	1,034	52
DBTs	883	24	782	39
Total	**3,691**	-	**1,999**	-

Other factors affecting the deposition of PACs, such as snow characteristics and distance to sources and wind, were evaluated using multilinear regression models. The majority of the variability was explained by ΣPAC concentrations measured in the snow pack (2012: 98 %, $p<0.05$; 2013: 97 %, $p<0.05$), with snow physical properties contributing 3 % or less (2012: 2 %, $p<0.05$; 2013: 3 %, $p<0.05$). Distance from main developments, by itself, explained 44 % and 39 % ($p<0.05$) in 2012 and 2013 respectively, which suggests that there are other PAC sources in the area. In addition, approximately 5 % of the total variability of ∑PAC loadings was explained by a combined model that included wind direction and wind speed in 2012 ($R^2=0.05$, $p=0.06$), and 8 % in 2013 ($R^2=0.08$, $p<0.05$).

∑PAC concentrations were found to be positively correlated with 13 priority pollutant elements (PPEs), total suspended solids (TSS), particulate organic carbon (POC), particulate organic nitrogen (PON), and crustal elements found in the snow pack. This included metals known to be emitted in large quantities from the upgrading facilities (e.g., nickel (Ni), vanadium (V) and zinc (Zn)). The high correlation of ∑PACs and metals such as V reinforces the origin of these PACs in relation to the major developments and the generation of particles from mining and land disturbances.

The presence of other factors potentially affecting deposition of PACs indicates that new potential sources should be explored. Further deposition monitoring and measurement of novel PACs that may be characteristic of sources are planned to address these questions. Additionally, future monitoring will include sampling sites with a more grid-like distribution around the area, which will be capable of capturing variations in concentrations and deposition at a local scale.

<u>THg, MeHg, and additional inorganic and organic contaminants:</u> Similar to PACs, concentrations and loads of THg, MeHg, and numerous other inorganic contaminants (e.g., Ni, V, Zn, Ni, Pb, TSS, Al, Fe, La, TSS) were highest near the major developments. Spring-time snowpack THg concentrations ranged from 0.8 to 14.4 ng/L with lowest concentrations observed in the PAD (n=9, average = 1.19±0.24 ng/L) as well as at numerous sites distant from major developments. Highest THg concentrations (>8 ng/L) were observed at 15 sites within the major Oil Sands development area, predominantly in the region between the Muskeg and Steepbank rivers. MeHg concentrations were also elevated in this area, reaching up to 0.27 ng/L and decreasing to concentrations just at or above the method detection limit of 0.015 ng/L in the PAD and at several distal sites (average = 0.016±0.002 ng/L in the PAD). Given that snow packs provide a direct measure of atmospheric deposition, these results suggest that oil sands developments are a source of airborne THg and MeHg emissions to local landscapes and water bodies. Generally, inorganic Hg(II) deposited in precipitation to landscapes and water bodies must undergo a methylation step before it can be taken up by organisms and biomagnified through food chains. Therefore, elevated MeHg levels in snow packs may be of particular relevance to aquatic and terrestrial ecosystems of the region. The THg and MeHg deposited to snow packs was predominantly bound to particulates >0.45 µm in size (79±12 and 72±18% particulate-bound, respectively), which may affect its transport, availability for uptake by organisms, and, ultimately, its impact on local ecosystems.

Similar to Hg concentrations, THg and MeHg loadings were elevated at many sites within the major development area, reaching up to 1420 and 19 ng/m^2, respectively, and decreasing to 103±42 and 1.2±0.2 ng/m^2, respectively, in the PAD (Fig. 3). As with PACs, THg and MeHg deposition maps were created by interpolating measured Hg loadings using ArcGIS geostatistical software (Fig. 3). As with PACs, the kriged interpolations produced deposition maps with areas of maximum THg and MeHg loadings located primarily between the Muskeg and Steepbank rivers and resembling a bullseye pattern on the landscape. This deposition pattern was consistent for numerous other parameters examined, including metals known to be emitted in large quantities from the upgrading facilities (e.g., Ni, V, and Zn), crustal elements (Al and La), and total suspended solids (TSS) (Fig. 3). Patterns in particulate-bound Hg deposition were similar, whereas dissolved THg and MeHg deposition was fairly low over the entire region (<200 and 3 ng/m^2, respectively). The deposition maps produced from our measured Hg loads suggest that in 2012, the region

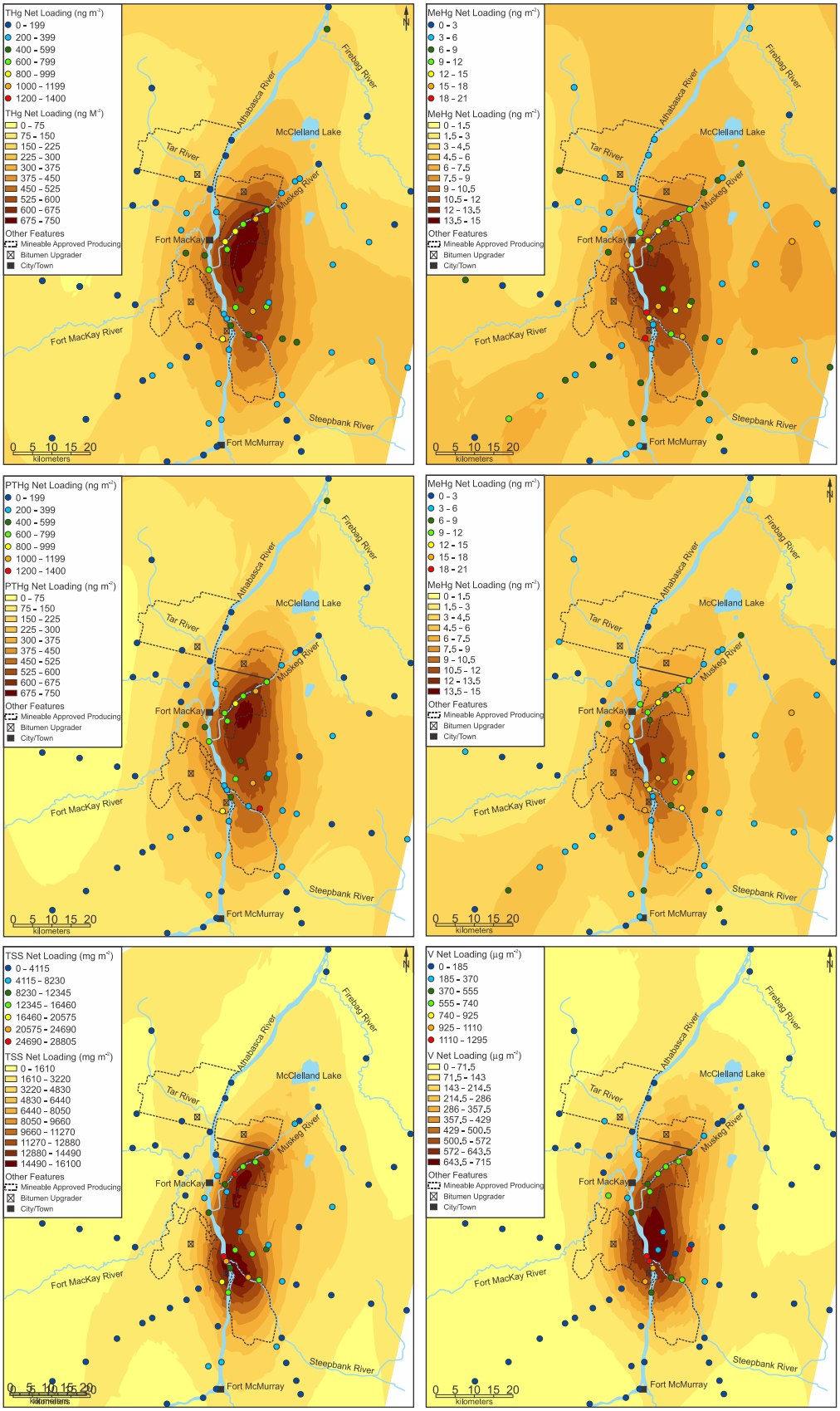

Figure 3. Deposition of THg, MeHg, particulate-bound THg and MeHg (pTHg and pMeHg, respectively) to the Athabasca Oil Sands region in winter 2012. Interpolated loads (ng/m^2) of each contaminant produced using ArcGIS Geostatistical Analyst software are overlain by measured loads (ng/m^2) at each site. Particulate-bound THg and MeHg loads were calculated by the difference between unfiltered and filtered loads.

of maximum deposition was centred <20 km from site AR6. Therefore, similar to Kelly et al. (2010), plotting measured Hg loadings versus distance from AR6 produced a roughly exponential decay relationship (Fig. 4).

THg and MeHg deposition at our most distant sites in the PAD averaged only 103±42 and 1.2±0.2 ng/m^2, respectively, which compares well to values observed using the flat portion of the exponential decay curve obtained from plotting THg and MeHg loads versus distance from AR6 (Fig. 4). Assuming that <100 and 1.5 ng/m^2 represent respective THg and MeHg loadings not affected by oil sands developments, our results suggest that almost the entire ~20, 000 km^2 sampling area where spatial coverage was sufficient to allow interpolation of Hg loadings is currently affected by airborne Hg emissions originating in the oil sands development area. Future sampling will therefore include numerous sites located further away from the major development area. Using average particulate-bound THg loads of 56±33 ng/m^2 in the PAD to represent baseline values, we estimate that ~16,800 km^2 is affected by Oil Sands-associated particulate-bound Hg emissions. Although our results suggest that Hg deposition is elevated above baseline for an area of ~20,000 km^2, both the deposition maps and plots of loadings versus the distance from AR6 suggest that Hg loads decrease fairly rapidly from maximum depositional zones. For example, for THg and MeHg, 89 and 80 %, respectively, of the ~20,000 km^2 area examined receive loads <half those observed in the maximum deposition zone (<300 and 6 ng/m^2, respectively). Similarly, plots of Hg loads versus distance from AR6 suggest that deposition decreases dramatically at ~50 km from AR6 (Fig. 4).

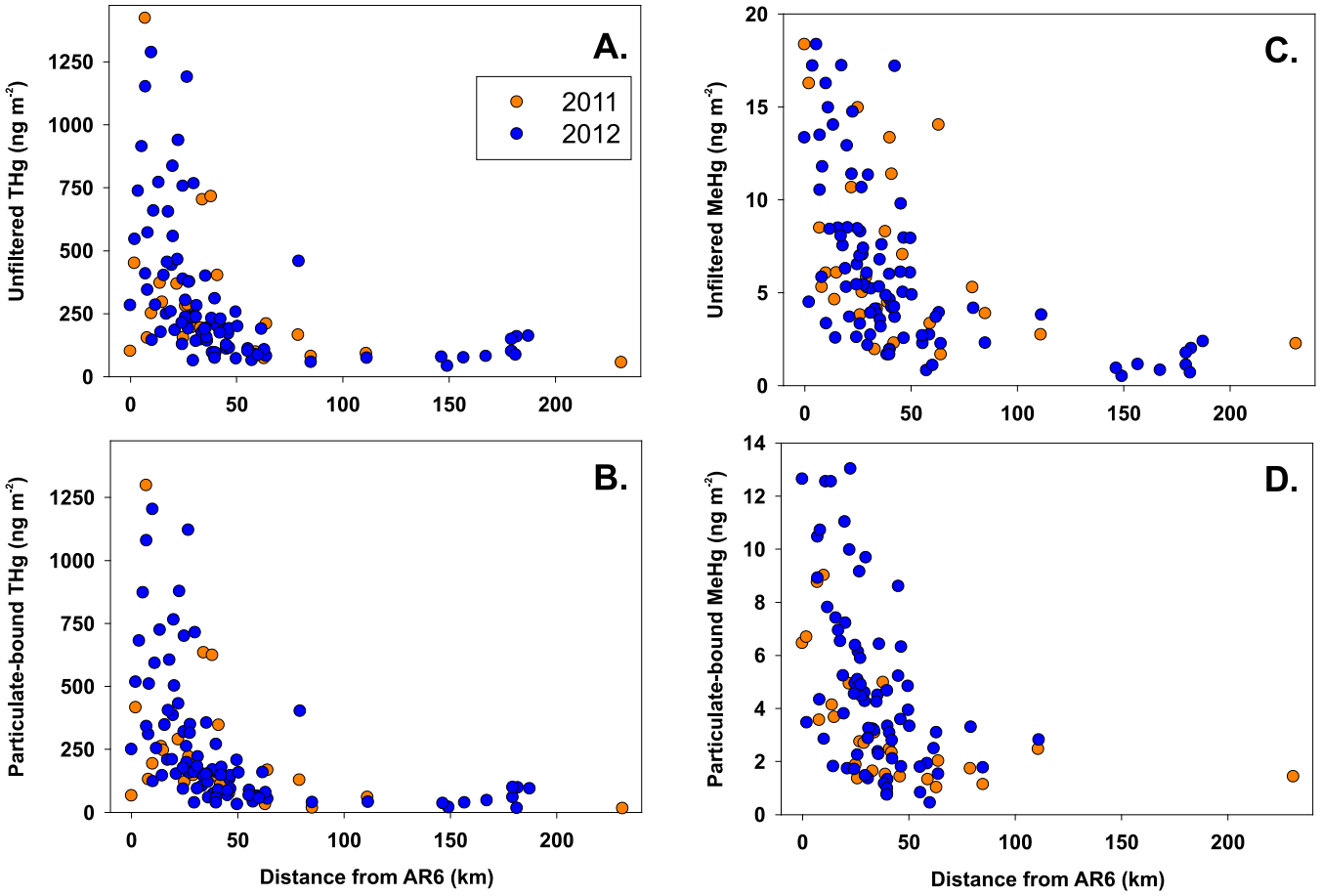

Figure 4. Winter 2011 and 2012 loadings (ng/m^2) of unfiltered THg (A) and MeHg (C), particulate-bound THg (B) and MeHg (D) versus distance from site AR6 in the Athabasca Oil Sands region.

As for PACs, relationships between Hg and snowpack characteristics, wind, and other chemicals were examined to identify potential factors driving the spatial patterns in Hg deposition. Concentrations and loadings of THg and MeHg and the other parameters examined were not normally distributed (Shapiro-Wilk normality test, $p<0.05$) and were thus log transformed prior to statistical analyzes. Multiple linear regression modelling demonstrated that Hg loadings were driven primarily by Hg concentration rather than by snowpack depth or snow water equivalence, with concentrations explaining 78 and 82 % of the variability in THg and MeHg loadings, respectively. These results suggest that local Hg emissions, and not precipitation quantity, drive Hg deposition to snow packs in the region. Distance from AR6 explained 41 and 48 % ($p<0.01$) of the variation in THg and MeHg loadings, respectively, suggesting that there are additional sources of atmospheric Hg emissions besides the upgraders near AR6, or that wind patterns affect the distribution of local Hg emissions. However, together wind speed, wind direction, and distance from AR6 explained only an additional 15 % of the variation in Hg loads than distance from AR6 alone (ANCOVA; $r^2=0.56$ and 0.63, $p<0.01$). Given that the majority of THg and MeHg in snow packs of the Oil Sands region was particulate-bound, we hypothesize that particulate-bound emissions to the atmosphere are rapidly deposited near local point sources.

THg and MeHg were significantly correlated with numerous water chemistry parameters and metals, including TSS, V, Zn, Ni, Pb, Al, Fe, La, TP, POC, and PON ($r=0.73$-0.86, $p<0.01$), which were also deposited to the oil sands region in large quantities (Table 2). Correlation coefficients between TSS, Ni, V, Zn and Ni, Pb, TSS, and Al, Fe and La ($r=0.79$-0.99, $p<0.01$), were consistently higher than between these parameters and THg and MeHg, suggesting that THg and MeHg are bound to different particles, potentially of different sizes, than other contaminants and thus undergo altered transport processes. Alternatively, THg and MeHg may undergo post-depositional processing in snow packs, likely by photoreduction and photodemethylation, respectively, as has been shown in numerous other systems (Durnford et al. 2011). Due to the important role of DOC in controlling transport of THg and MeHg, as well as rates of Hg(II) methylation to MeHg in aquatic ecosystems, Hg and DOC are often tightly correlated in lakes and rivers (Driscoll et al. 1994, Ullrich et al. 2001, Driscoll et al. 2013, Dittman et al. 2010). Significant relationships between Hg and sulphate are also often observed as sulphate can control Hg(II) speciation and Hg(II) methylation rates by sulphate reducing bacteria, which are often the principal methylating bacteria present in aquatic ecosystems (King et al. 2000, King et al. 2001). Sulphate and DOC deposition was elevated in snow packs of the Athabasca Oil Sands region. However, correlation coefficients between both THg and MeHg and DOC and sulphate were lower ($r=0.45$-0.54, $p<0.01$) compared to those observed between the metals and other water chemistry parameters examined, suggesting differing sources of THg and MeHg versus DOC and sulphate to local snowpacks.

Potential sources of MeHg to snowpacks: MeHg may be produced *in situ* in snow packs by methylation of deposited Hg(II). However, all current proposed mechanisms are specific to Arctic coastal snow packs and therefore invoke the presence of marine air masses or sea spray for MeHg production (Constant et al. 2007, Barkay et al. 2010, Larose et al. 2010). Hg(II) methylation in precipitation prior to deposition is also possible (Hammerschmidt et al. 2007). However, to produce the almost identical bullseye patterns in THg and MeHg deposition for winter 2012, methylation rates would need to be consistent over the entire region examined. This seems unlikely, since methylation rates are a function of both the quantity of bioavailable Hg(II) present in the environment and the activity of microorganisms carrying out Hg(II) methylation (Hintelmann et al. 2010), which in turn is dependent on energy sources for microbes and redox conditions. Further, the %MeHg, an indicator of active methylation in aquatic ecosystems (Kelly et al. 1995, Rudd et al. 1995), was quite low (average 2.5±1.7 % in 2012), and varied from site to site throughout the entire sampling region. Finally, the positive significant relationships observed between MeHg and other contaminants known to be emitted from Oil Sand-related processes (for example, V, Zn, and Ni) suggest that MeHg is also released directly to the atmosphere from industrial processes. Consequently, measurement of MeHg from various potential emission sources is

warranted. Examination of Hg transformations in snow packs, including potential rates of Hg(II) methylation, using amendments of snowpacks with enriched Hg stable isotope tracers as has been carried out in lake waters (Eckley et al. 2006) would also be informative.

Short-term (2008-2013) temporal trends in contaminant deposition: The availability of PAC concentrations and loadings for the period 2011-2014 allowed us to develop the first temporal trend data for PAC deposition in the region. We compared results with those reported by Kelly et al. (2009) for 2008, and noted how they have changed in relation to cumulative emissions associated with growing bitumen extraction and crude oil production (Fig. 5). Only sites located at the same geographical coordinates as in 2008 were used along with the same PAC analytes (n=41 in each year, Σ_{41}PAC). PAC diagnostic ratios did not change from year to year ($p>0.05$), suggesting that PACs in the Athabasca Oil Sands came from the same sources from 2008 to 2014. The Σ_{41}PAC mass deposition generally increased from 2008 to 2012. However, a decline was observed for 2013 (Fig. 5). The estimated PAC mass deposition was positively correlated with the oil production in the area; however, the increase in measured PACs was closer to the trend shown by NPRI reported emissions, rather than to a constantly growing production rate (Fig. 5).

Comparison of winter-time deposition estimates to contaminant emissions data reported to the National Pollutant Release Inventory (NPRI): We compared deposition estimates for the area within 50 km of the major developments (ob-

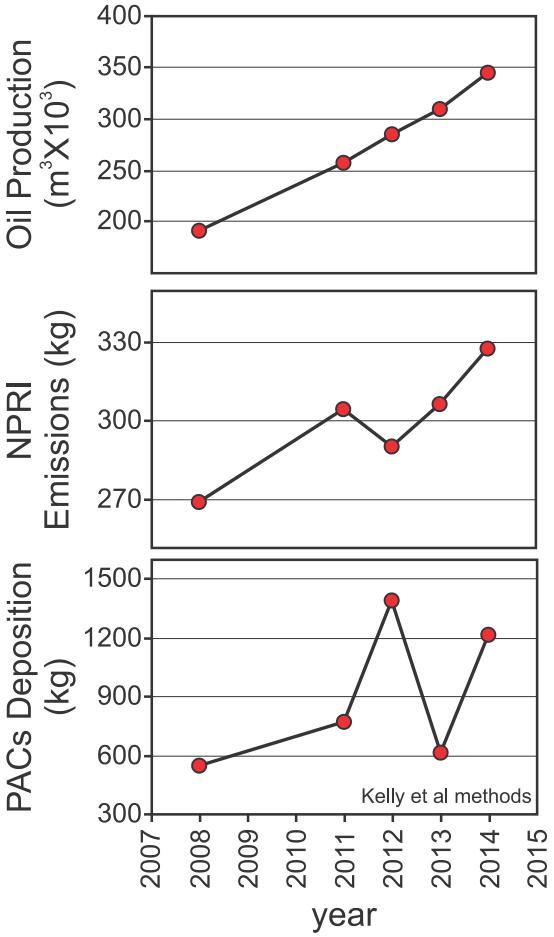

Figure 5. Short-term temporal trends (2008-2014) in PACs deposition, oil production, and total PACs emission data reported to the National Pollutant Release Inventory (NPRI) for the Athabasca oil sands industry. Note that the PAC deposition is based only on the sites used by Kelly et al. (2009).

tained from our kriged deposition maps) to airborne emissions reported to NPRI for the region for the year 2012 and to estimated winter 2012 emissions. Winter 2012 emissions were estimated by weighting annual emissions for the number of days of winter 2012. NPRI reports include 21 PACs, mostly unPACs, and estimated that 290 kg (2012) and 306 kg (2013) were emitted in the oil sands region (NPRI, 2014). Considering only the PACs reported by NPRI, we estimate that PAC winter deposition within 50 km of the main developments was 215 kg (2011) and 98 kg (2013). If NPRI estimates do in fact capture all major PACs emission sources, it would mean that between 32 % and 74 % of total annual PACs emissions originated over the four winter months, which seems unlikely. This comparison highlighted that NPRI emissions are underestimated, and/or, there are other airborne emissions besides the upgrading facilities that contribute to deposition of PACs in this region that are not required to be publicly reported. Potentially important sources could include emissions of particulate material from mining activities, petroleum coke particles stored at the upgrading facilities, various land disturbances and activities that can produce flying dust, such as mine haul road materials, and vehicle emissions that are also related to industrial activities (Graney et al. 2012, Zhang et al. 2016).

Interpolation of measured THg, MeHg, TSS, V, Zn, and Ni loadings for the area within 50 km of AR6 produced deposition estimates of 1.9 and 0.05 kg, 25, 800 T; 3000, 8560, and 1460 kg, respectively, for winter 2012 (November 15, 2011 to March 6-10, 2012) (Table 2). Assuming airborne emissions do not vary greatly among seasons, comparison of emissions data with winter-time loadings for the region within 50 km of AR6 suggests that the airborne emissions reported to NPRI are underestimated, especially for Zn (Table 2). Kelly et al. (2010) also reported high loadings of airborne particulates to snow packs of the Oil Sands region and by extrapolation of the observed exponential relationship between TSS loadings and distance from, estimated that 11,400 metric T of

Table 2. Winter 2012 loads of THg, MeHg, total suspended solids (TSS), total phosphorous (TP), total nitrogen (TN), particulate organic nitrogen (PON), vanadium (V), zinc (Zn), nickel (Ni), aluminium (Al), and iron (Fe) to landscapes and water bodies within 50 km of AR6, as well as oil sands industry airborne metals emissions as reported to the National Pollutant Release Inventory for the Athabasca oil sands region for 2011 and 2012 (NPRI).

Contaminant	Winter 2011-2012 loads within 50 km of AR6	Annual 2011 airborne emissions as reported to NPRI	Annual 2012 airborne emissions as reported to NPRI	Estimated 2012 winter emissions[1]
	(kg or T*)	(kg)	(kg)	(kg)
THg	1.9	52	52	16
MeHg	0.05			
TSS	25 890*			
TP	28.6*			
TN	463*			
PON	153*			
V	3000	5048	5140	1594
Zn	8560	2957	3492	1022
Ni	1470	2444	2962	858
Al	793*			
Fe	2150*			

[1]Winter 2012 emissions were estimated by weighting annual emissions for the number between the first snowfall (November 15, 2011) and snowpack sampling (March 7, 2012; n= 47 and 67 days in 2011 and 2012, respectively).

*refers to metric Tonnes

suspended solids were deposited to the area within 50 km of AR6 over winter 2008. Using a geostatistical approach, which likely captured the spatial heterogeneity in contaminant deposition more accurately, we estimate a 2012 winter-time TSS loading of ~25,800 T. Interestingly, unlike PACs, V, Zn, Ni, and THg, loads are lower within 50 km of AR6 than what is reported to NPRI from the upgraders in the region. These results suggest that post-emission transport and post-depositional processing are different for THg than for many of the other contaminants. For example, Hg may be emitted primarily from the upgrading facilities as gaseous elemental Hg(0), which is stable in the atmosphere and thus undergoes long-range transport.

2.3 Summary and Conclusions

Results of the 2011-2014 JOSM snowpack program make clear that a variety of contaminants, including PACs, metals, THg, MeHg and a variety of other inorganic contaminants (TSS, TP, POC, and PON) are deposited via wet and dry deposition to the oil sands region. These results suggest that at snow melt, a complex mixture of chemicals enters aquatic ecosystems and could affect biological communities. A large proportion of the contaminants measured in snow packs located close to the major developments was particle-bound, which may affect its transport and fate in aquatic and terrestrial ecosystems. Interpolation of 2012-2014 measured snowpack loadings using ArcGIS10© geostatistical software allowed us to produce deposition maps to examine spatial patterns in contaminant deposition. These maps demonstrated that in winter 2012-2014, deposition was highest near the major development area, with areas of maximum deposition covering parts of the Athabasca, Steepbank and Muskeg rivers. Contaminant deposition decreased rapidly with distance from the major development and was found to be close to background beyond 50-75 km; however, more distant sites, such as those obtained from snowpack sampling in 2015, and sensitive methods are needed to fully characterize background and potential inputs from the oil sands for this region. No clear temporal trend was observed in snowpack loadings from 2008 and 2011-2014, suggesting additional annual snowpack monitoring is needed. Interpolated snowpack loadings were used to estimate contaminant loads to the region within 50 km of the major development area and were then compared to NPRI emission estimates. Results of these comparisons suggest that emissions not reported to NPRI, such as fugitive dusts (e.g., mining, tailings, on/off roads, etc.) are important contributors to contaminant deposition in the Athabasca Oil Sands region.

The snowpack study presented here was designed to integrate with other JOSM components. For example, PACs and metals analyte lists for snowpack measurements were the same as those for the water quality, air, invertebrate, fish and wildlife monitoring programs so that data can be integrated. In addition, snowpack samples were collected at air, invertebrate and fish and wildlife monitoring sites so that contaminant loads at these different monitoring sites can be provided to various program partners. Finally, comprehensive sampling was carried out on the Steepbank, Muskeg and Ells rivers so that catchment contaminant loadings to these rivers can be determined. Projects have been initiated to integrate atmospheric deposition measurements derived from snowpack measurements with hydrology and water quality measurements to determine how aerial deposition to the landscape affects water quality in the tributaries and Athabasca main stem.

3. Long-term (~100 years) Trends in Atmospheric Deposition of Contaminants

This sub-component uses highly resolved, dated sediment cores collected from 25 lakes located 10-185 km from the major development area to determine long-term temporal trends (over the last ~100 years) in atmospheric deposition of PACs and numerous elements to lakes of the Athabasca Oil Sands region. To quantify changes in PACs and multi-elements, including metals, deposition since development began in the ~1960s, we used a series of change indices, including enrichment factors (EFs), fluxes (F), and flux ratios (FR). We used a series of PACs diagnostic markers and ratios to assess changing PACs sources over time, including DBTs/chrysene and methylphenanthrenes/phenanthrenes ratios, which are indicative of petrogenic influence. To assess changes in metals deposition through time, we corrected all sediment metals concentrations and flux data for watershed/geologic metals inputs by normalization to lithogenic element aluminum, then carried out principal component analyzes (PCA) to identify sources of variation in the multi-element data.

To examine changes in contaminant deposition within the context of climate-induced changes to lake limnology within the region, we carried out analyzes of dated sediment cores for VRS chlorophyll *a* (chl *a*) and algal and invertebrate fossil remains. VRS-chl *a* is a fairly new and non-destructive technique that measures all degradation products and is therefore not affected by diagenetic processes (Wolfe et. al. 2006, Michelutti et al. 2010). Here we present VRS-chl *a* results from 23 dated lake sediment cores collected between 2012-2014, including breakpoint analyzes to assess the timing of shifts in lake primary production, and correlation analyzes between VRS-chl *a* data and climate data, including mean annual and seasonal temperature and precipitation data for the region. To examine the potential effects of development and other environmental stressors on biological assemblages in oil sands lakes, crustacean zooplankton (*Cladocera*) assemblages from five sediment cores collected in 2011 were enumerated. Data analyzes of diatom and zooplankton fossil remains in additional cores are on-going.

3.1 Methods

Study design

From 2011–2015, intact sediment cores were collected from the deepest point of 28 lakes (Fig. 6). A sediment core collected in Namur Lake collected in 2009 was also included. Except for lakes Gregoire, Namur, LaLoche and Peter Pond, which were relatively large (2,580-55,200 ha surface area), all were small, single-basin lakes (4–575 ha); these types of systems have been shown to be good recorders of past atmospheric deposition. The study lakes were located between 10 and 185 km from site AR6, the snow sampling site named by Kelly et al. (2009) near the major oil sands developments, providing a spatial gradienzzt away from oil sands mines.

Three cores were collected from each lake. All cores were collected through holes drilled through the ice using a Uwitec gravity corer, as described in Kurek et al. (2012), during March each year. After collection, cores were returned intact by helicopter to Fort McMurray airport. They were sliced within 1 to 5 hrs of collection at 0.5-cm intervals for the top 20 cm and at 1-cm intervals for the bottom 20-40 cm so that high resolution (~5-10-year time scales) records of contaminant deposition could be obtained. Samples were placed in polypropylene jars with screw capped lids or Whirlpak® bags and frozen for transport.

Sample Analyzes

^{210}Pb dating of sediments: Sediment ages were estimated by Flett Research Ltd. (Winnipeg, Manitoba, Canada) using standardized radioisotopic methods (Appleby 2001). Alpha radiation of ^{210}Po was measured as a proxy for total ^{210}Pb activity, and background ^{210}Pb levels were determined through measuring alpha radiation of ^{226}Ra. Radioactivity of ^{137}Cs was measured with gamma spectrometry and was used as an independent chronological marker of the radioactive fallout peak following the 1963 moratorium on nuclear weapons testing (Appleby 2001). The constant rate of supply (CRS) model (Appleby 2001) was used to determine the ages of the measured sediments over the constant initial concentration (CIC) model as

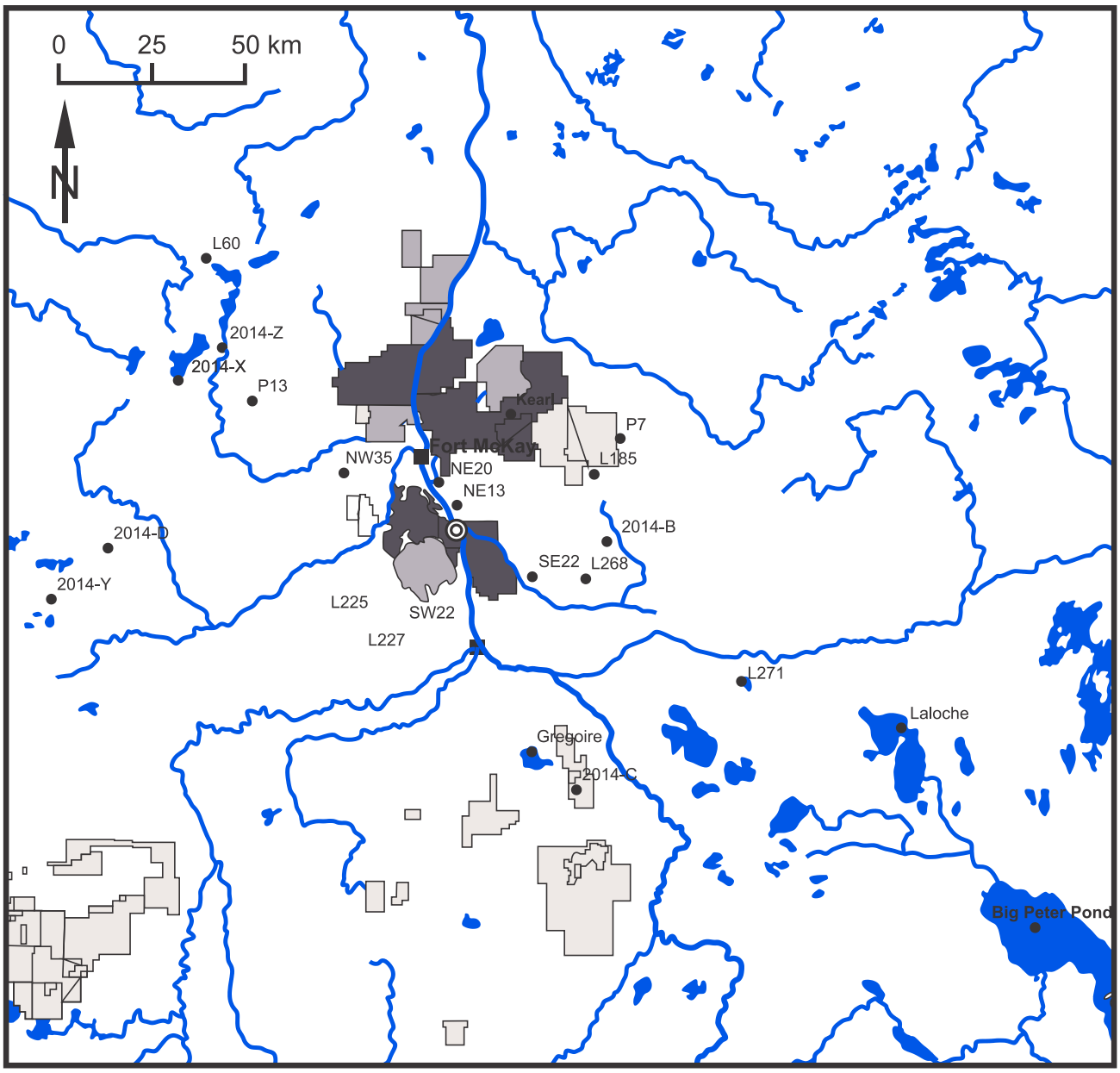

Figure 6. Locations of 23 study lakes and two local communities (Fort McMurray and Fort McKay), and the footprint of industrial oil sands development. Lakes were cored in either March 2011, 2012, 2013, or 2014.

the former can accommodate sediment core profiles with non-monotonically declining ^{210}Pb profiles (see Fig 7d) indicative of changing sedimentation rates within a lake's history. The ages for the remaining sediment intervals were interpolated and extrapolated from second, third, and fourth-order polynomial curves fitted to the dated sediment intervals age-depth relationships with the intercepts set to the time of coring (Summers et al. 2016). Here, we present ^{210}Pb dating results on the 25 sediment cores collected between 2011-2014. Analyzes of the 2015 cores are currently underway.

PACs in sediments: PACs analysis of lake sediments was conducted on 20 to 25 sediment sections from each core by AXYS Analytical Services Ltd. (Sidney BC) using their method MLA-021, which is based on US EPA Methods 1625B and 8270C/D. Each sample was defrosted in the analytical laboratory and homogenized by manual stirring. An accurately-weighed subsample was then dried with anhydrous, powdered Na_2SO_4. The dried subsample was spiked with a suite of 16 perdeuterated surrogate PAC standards and Soxhlet extracted with dichloromethane (DCM) for 18 hours. A second subsample was then oven dried to determine moisture content.

The extract was concentrated to ~2 mL and exchanged into hexane for clean-up. The extract in hexane was fractionated on a silica column with pentane for the first discard fraction and dichloromethane for the second PAC fraction. The PAC fraction was subjected to Alumina clean-up using hexane for the first discard fraction and DCM for the second PAH fraction. This extract was analyzed, after concentration and addition of a recovery standard containing perdeuterated acenaphthene, pyrene, and benzo(e)pyrene, by low-resolution mass spectrometry (LRMS) using an RTX-5 capillary GC column. The LRMS was operated at a unit mass resolution in the electron impact (EI) ionization mode using multiple ion detection, acquiring at least one characteristic ion for target analytes and surrogate standards. Concentrations of PACs were calculated using the isotope dilution method of quantification. Most C1-C4–alkylated PACs were determined as a group using response factors based on a multipoint calibration using selected individual alkylated PAH standards, whereas other alkylated PAHs were determined by single-point calibration. Average recoveries of 19 individual unPACs and 24 aPACs ranged from 86 to 117 %. All results were blank corrected using the blank from the batch of 20 samples. Method detection limits (MDLs) were calculated as 3× SD of blank results or where no analyte was detected in the blanks, on the instrument signal-to-noise ratio of 10. MDLs were generally <10 ng/g based on 0.5 g dry wt., except for naphthalene (13.5 ng/g) and biphenyl (11 ng/g). Among the C1-C4–alkylated PAH analytes, eight had MDLs in the range of 10–46 ng/g, whereas C2-biphenyl and C2-naphthalene had MDLs of 334 and 108 ng/g, respectively (Kurek et al. 2013). Results reported at less than the MDL were replaced with half the detection limit, except for blank results where nondetects were replaced with zero. Here we present PACs results on 25 of 28 dated lake sediment cores collected between 2011-2014; analyzes of the cores collected in 2015 is on-going. A certified reference material for PAHs (National Institute of Standards and Technology (NIST) SRM 1944, an urban/marine sediment, was used for every 20-25 samples.

Multi-elements in sediments: Between 20 and 25 intervals from each sediment core were analyzed for the concentration of 45 elements using standard analytical protocols at the National Laboratory for Environmental Testing. The method used (HMARSOIL-E3062A by the Ontario Ministry of the Environment) deliberately targets those elements weakly bound to organic and inorganic particles and not those elements directly incorporated into mineral lattices (Graney et al. 1995, Gobeil et al. 2013) and allows for the direct comparison to Canadian Council of Ministers of the Environment (CCME) sediment quality guidelines (CCME 2001). Elemental concentrations were quantified using an Inductively Coupled Plasma Mass Spectrometer (ICP-MS). Every core slice was analyzed for THg concentration at the CCIW Low-Level Analytical Laboratory using thermal decomposition, pre-concentration and atomic absorbance spectrophotometry (Milestone DMA-80 direct Hg analyzer). Standard Reference Materials TORT-2 (lobster hepatopancreas, National Research Council (NRC)), MESS-3 (marine sediment, NRC), SRM-2976 (mussel, National Institute of Standards and Technology (NIST)) and SRM1556b (oyster, NIST) were analyzed with each batch of 30 samples. Here we present metals results on 12 of 28 dated lake sediment cores collected between 2011-2013; analyzes of the cores collected in 2015 are on-going.

Visual reflectance spectroscopy chlorophyll *a* (VRS-chl *a*): Visual reflectance spectroscopy (VRS) was used to estimate concentrations of sedimentary chl *a* as described in (Wolfe et al. 2006, Michelutti et al. 2010, Kurek et al. 2013, Summers et al. 2013). A subsample of each core slice was first sieved through a 125-µm mesh. The spectral reflectance of ~2-3 mm of sediment in a 19x65 mm glass vial at a 650–700 nm spectral signature was then analyzed using a FOSS NIRSystem Model 6500 rapid content analyzer. The detection limit of the method is 0.01 mg/g dry weight. An inference model was applied to the spectral data to generate VRS-chl *a* concentrations for each sediment interval (Michelutti et al. 2010). Here we present VRS-chl *a* results on 23 of 28 dated lake sediment cores collected between 2011-2014.

Cladoceran fossil remains: To examine the potential effects of oil sands development and other environmental stressors on biological assemblages in oil sands lakes, crustacean zooplankton (Cladocera) assemblages from the five sediment cores collected in 2011 were enumerated. Cladocera are key algal grazers positioned centrally in aquatic food webs (Dodson et al. 2001) and respond more directly to local, environmental gradients rather than predation

or dispersal-related factors (Kurek et al. 2011). Standard guidelines for processing and counting cladocera were followed (Korhola et al. 2011) to ensure that assemblages were characterized adequately (Kurek et al. 2010). Numerical techniques of indirect ordination and constrained clustering were used to summarize the main variation in the multi-species cladoceran assemblage data through time. Data analyzes of diatoms and zooplankton remains in cores collected during 2012-2015 are on-going and will be included in future assessments.

Data analysis

Calculation of PACs and metals fluxes, flux ratios and enrichment factors: To quantify changes in PACs and metals deposition since oil sands development began in the region, a series of change indices was calculated, including enrichment factors (EFs), fluxes (F), and flux ratios (FR).

For PACs, total PACs (ΣPACs) represented the sum of 46 analytes (i.e., 17 unsubstituted PACs (unPACs), 24 C1-C4 alkylated PAHs (aPACs), and five dibenzothiophenes (ΣDBTs)). Perylene was not included in the sum of total PACs because it increased down core and is naturally produced in sediments (Yunker et al. 2003).

For metals data, prior to any calculations, metal concentrations in each core were first normalized to aluminum (Al). The geochemical record preserved in lake sediments reflects not only atmospheric deposition but inputs from the surrounding watershed. Using lake sediment cores as archives of past atmospheric metal deposition therefore requires estimation (and subtraction) of watershed inputs. Here we accomplish this by normalizing metal concentrations to the lithogenic element Al. This normalization accounts for changes in mineral input and also allows us to control for grain-size effects. It is a common practice when working with both fluvial (Wiklund et al. 2014) and lacustrine (Boës et al. 2011) systems, and when working with other types of environmental archives including peat cores (Shotyk et al. 2002) and ice cores (Krachler et al. 2009).

After normalization (for metals only), PACs, element and VRS chl *a* enrichment factors, which compare contaminant concentrations for the period before oil sands development began (pre-1970) to recent times (post-1990), were also calculated as:

$$EF = \text{recent}_{(\text{post 1990})} / \text{pre-industrial}_{(\text{pre 1970})} \quad (3)$$

concentrations.

Concentrations of contaminants within lake sediments are influenced not only by input of contaminants, but also by changes in lake sedimentation rate. To account for this, we calculated PACs and element accumulation rates or fluxes using the formula:

$$F\ (\mu g/m^2/y) = \text{Concentration}\ (\mu g/g) \times {}^{210}\text{Pb-derived sedimentation rates for each core horizon}\ (g/m^2/y) \quad (4)$$

Anthropogenic PACs and metal fluxes (ΔF), or the change in flux between before oil sands development began and recent times, and flux ratios were also calculated as follows:

$$\Delta F\ (\mu g/m^2/y) = F_{recent} - F_{pre\text{-}ind} \quad (5)$$

(pre-industrial)

$$FR = F_{recent}/F_{pre\text{-}ind} \quad (6)$$

PACs were decadally averaged for near field (10-50 km from AR6) and far-field (60-185 km) lakes by combining sampling horizons within the same date range (10 years from 1900-1970, five years from 1970 to 2015). Maximum post-2000 enrichment factors (EFs) were calculated as the ratio of fluxes in the most recent horizons (2000-2014) to the average pre-1970 flux.

For VRS-chl *a* concentrations, Z scores were calculated to facilitate comparisons of inferred primary production among lakes to standardize the data.

Statistical analyzes: Elemental data for each lake were included in a principal component analysis (PCA). PCA reduces the dimensionality of a data set in which there are a large number of interrelated variables, while retaining as much as possible of the variation present within the data set. Elemental data were centered and standardized prior to inclusion in the PCA, and two separate PCAs were conducted, the first including all study lakes and the second excluding L60 and Gregoire Lake.

To characterize the timing of VRS-chl *a* increases, piece-wise linear regression models were applied to the VRS-chl *a* concentration data (SigmaPlot Version 10). A linear relationship with a single break point was assumed, and a two-segmented model was used. An ANOVA table and corresponding F test statistic from a null model was used to evaluate the statistical significance for each regression model. Breakpoint analyzes were not completed on lakes where no stable baseline was captured (RAMP 175, RAMP 226, and 2014-B), where outliers would drive the timing of the break point (Big Peter Pond). Pearson correlation analyzes were carried out on VRS-chl *a* Z scores versus mean annual and seasonal air temperature (Fort McMurray, station no. 3062696) and precipitation (Fort McMurray, station no. 3062693) data from Environment Canada's Adjusted and Homogenized Canadian Climate Data website (www.ec.gc.ca/dccha-ahccd). Given down-core sediment compaction and variation in sediment accumulation rates, temporal resolution of samples is reduced down core. To ensure each interval represented comparable amounts of time, the VRS-chl α Z scores and climate data were averaged across 5-year intervals.

3.2 Results and Discussion

Core chronologies: Age-depth models for 25 of the 28 sediment cores recovered have been developed using the ^{210}Pb dating information and results for the remaining three cores are pending (Fig. 7). Most sediment cores extend back 100 years or more, except for Kearl and Gregoire Lakes, which are limited to the past ~50 and ~45 years, respectively (Fig. 7). Recent sedimentation rates exhibit a high degree of spatial variability, spanning an order of magnitude ranging from <100 g/m^2/y to ~1,000 g/m^2/y. These results are broadly consistent with previous studies from the region (Hazewinkel et al.2008; Jautzy et al. 2013 Laird et al. 2013).

Historical profiles of PACs: All sediment records showed significant (Mann-Kendall trend test, all $p<0.05$) increases in ΣPAC concentrations and fluxes. C1-C4 aPACs and DBTs predominated in all sediments, representing 55 to 89 % and 1.8 to 17 % of the ΣPACs, respectively. However, the near-field and far-field lakes show different PAC depositional histories. The aPACs and ΣDBT predominated in recent sediment horizons of the 12 near-field lakes, i.e., aPACs >> ΣDBT > unPACs (Fig. 8). The proportions differed in recent horizons of far-field lakes; aPACs predominated but unPACs were more prominent than ΣDBTs. Decadally averaged fluxes of unPAC, aPAH and ΣDBTs in lake sediment cores from near-field areas all increased from the mid-20th century to modern times (Fig. 8). The timing of the increases of all three groups above "natural" background levels began at approximately 1970.

In near-field lakes, maximum EFs for ΣPAC of post-2000 sediments from pre-1970 background levels ranged between ~1.2 (L227) to 17 times (NE20) (Table 3) but much larger enrichments were observed for ΣDBTs (2.3–57) and aPACs (1.3-24). EFs for ΣPACs in far field lakes ranged from 0.7 (L2014X) to 9.2 (L13/175), from 1.3 (L6/271) to 54 (2014C) for ΣDBTs and from 0.7 to 9.8 (2014X to L13/175) for aPACs. The very high EF for ΣDBTs in L2014C is an anomaly, as the EF for other far field lakes ranged only up to 13. It was due to very low pre-1970 concentrations compared to most other lakes and a sharp increase post 2000. Thus, while the far-field lakes show overall much smaller EFs, the 60-km cutoff that we have used to define these lakes may not be appropriate. An 80-km threshold would give EFs for ΣDBTs ranging from 1.3 to 8.

Retene (RET), a marker of biomass combustion and terrestrial plant inputs (Yunker and Macdonald 2003) was a major individual PAC in sediments, with concentrations similar to total unPACs and ΣDBTs. RET showed no significant increase from pre-1960 to post-2000 time periods (Fig. 8). The 1,7-dimethylphenanthrene (MePH)/(1,7 + 2,6-MePH) ratios were >0.8 in pre-1970 sediments from all 25 lakes (Table 4), also implying wood-combustion sources (Yunker and Macdonald 2003). Post-2000 1,7-MePH/(1,7 + 2,6-MePH) ratios were lower (0.72) in near-field sediment cores, although still reflecting a wood combustion source.

PACs in post-2000 sediments had diagnostic ratios (e.g., DBTs/chrysene, methylphenanthrenes/phenanthrenes) indicative of greater petrogenic influence after oil sands development began in this region (Table 4). The source of the petrogenic PACs to the near-field lakes (which all have only atmospheric sources) could be both upgrader-related and dust particles from mining and land disturbance.

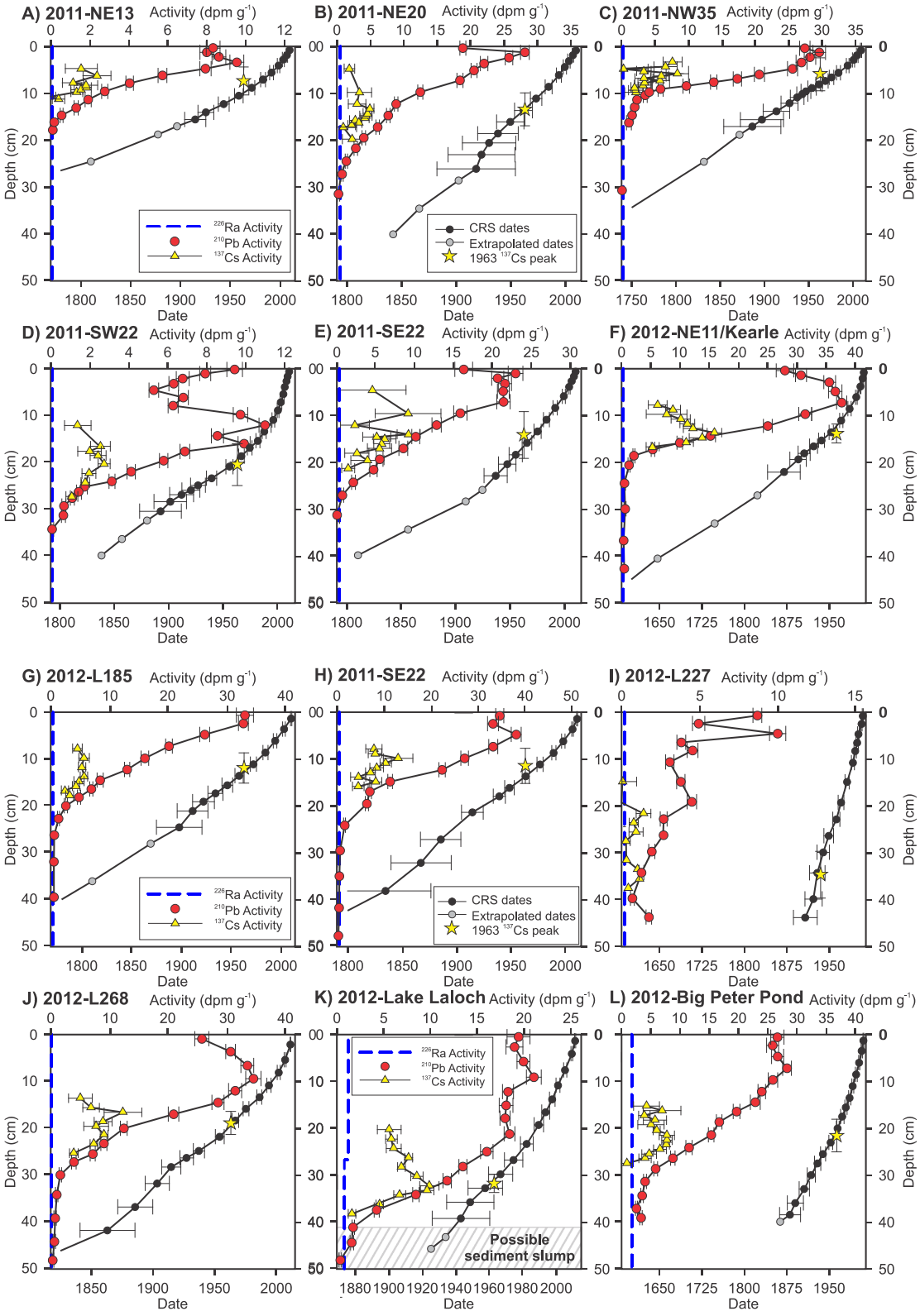

Figure 7. Lake sediment core profiles of supported (^{226}Ra activity) (blue dashed line) and total ^{210}Pb activity (red circles) and ^{137}Cs activity (yellow triangles) (± 1 SD), and age-depth models (black and light grey circles) for 23 sediment cores. Black circles represent constant rate of supply (CRS)-inferred dates; light grey circles represent extrapolated dates. Age-depth models were developed using the depth midpoint of sediment intervals, the CRS-inferred age, and polynomial regression (second, third, or fourth-order) with intercept set to the time of coring. The star overlain on the CRS dates denotes the depth of the 1963 ^{137}Cs peak. Profiles are ordered by year of core collection.

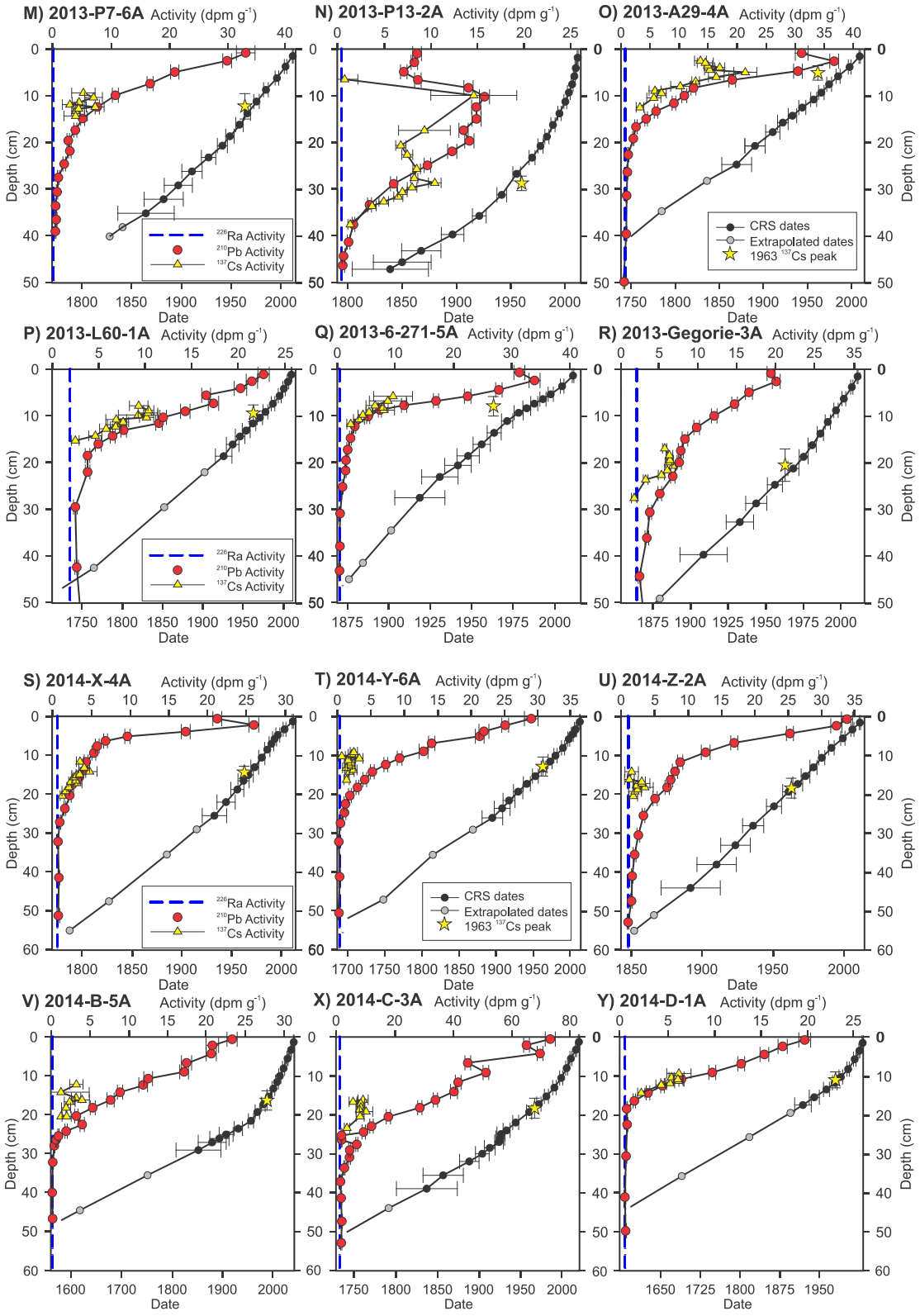

Figure 7. Continued

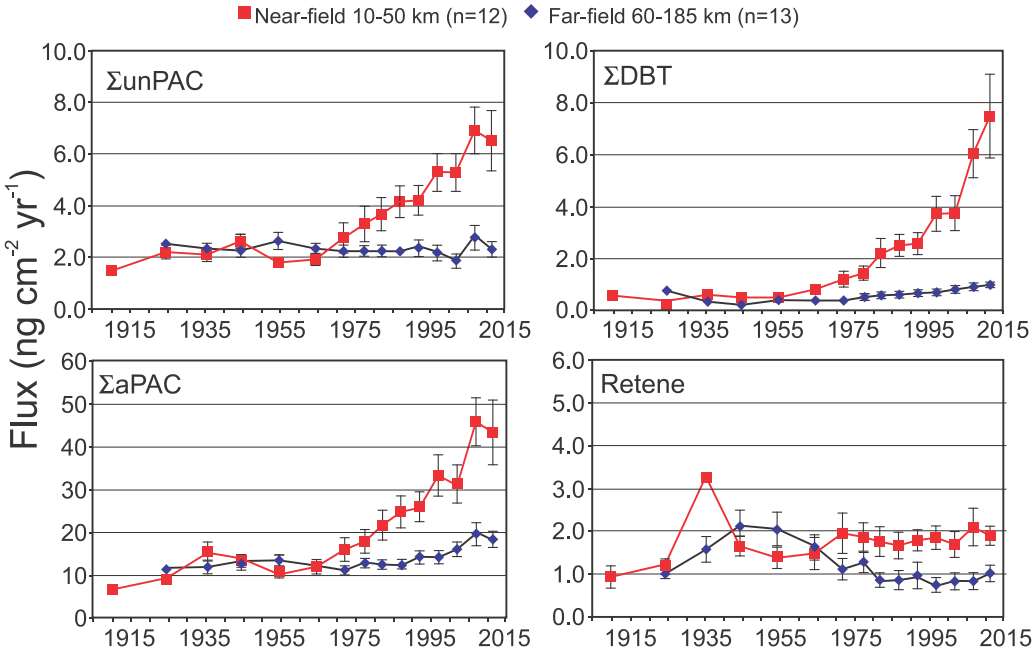

Figure 8. Decadally averaged fluxes of unPAC and aPAH and ΣDBTs in lake sediment cores from near-field (red squares) and far-field (blue circles) lakes.

Table 3. Lake characteristics and maximum post-2000 PAC enrichment factors.

			Enrichment factors				
Lake	Km from AR6	Lake surface area (ha)	ΣPAC	unPAC	aPAC	ΣDBTs	retene
Near field							
NE13	10	5	4.7	4.2	4.2	4.6	0.9
NE20	16	5	18	25	24	57	2.2
SE22	22	4	5.7	7.3	6.8	21	0.6
SW22 (226)	26	20	5.5	5.5	5.2	12	0.8
L227	31	9	1.2	1.4	1.3	2.3	1.3
NW35	33	10	2.2	4.8	5.1	13	0.6
Kearle	35	575	2.3	5.0	4.4	24	0.7
L268 (E15)	35	189	4.4	7.0	6.9	40	2.7
L225	36	23	3.8	6.5	6.8	33	1.3
L185 (ALB21b)	39	11	3.5	3.9	3.4	33	2.1
P7 (209)	50	11	1.9	0.5	2.0	19	0.7
2014-B	41	25	5.9	9.3	4.8	49	1.6
Far field							
L6 (271)	75	419	1.3	1.5	1.2	1.3	1.5
Gregoire	61	2580	3.7	0.7	4.0	6.7	1.2
L13 (175)	64	39	9.2	6.0	9.8	17	1.4
Namur	85	4322	7.1	7.7	7.6	13	4.3
A29/L167	92	106	1.1	2.0	1.0	1.9	0.9
L60	100	97	2.7	0.4	2.8	8.3	4.6
La Loche	125	20,600	1.3	0.9	1.4	2.0	0.5
Peter Pond	185	55,200	1.6	0.2	2.0	1.5	0.2
2014-C	75	25	7.5	2.7	7.9	54	4.1
2014-D	94	4	1.8	1.5	1.8	4.4	1.1
2014-Y	108	25	1.6	0.6	1.6	3.4	1.0
2014-X	84	25	0.7	0.3	0.7	4.0	3.6
2014-Z	79	143	2.1	1.1	2.2	11	0.9

Table 4. Diagnostic PAH ratios comparing averaged concentrations in pre-~1970 sediment intervals to averaged concentrations in post-2000 sediment intervals.

Diagnostic indicator	FF		FF		NF		NF	
	pre-1970		post-2000		pre-1970		post-2000	
	Mean	SD	Mean	SD	Mean	SD	Mean	SD
Ant/phe ratio	0.06	0.05	0.09	0.09	0.27	0.27	0.23	0.22
Flur-pyr ratio	0.39	0.10	0.48	0.15	0.55	0.14	0.50	0.20
ΣD (DBT.chry ratio)	0.42	0.47	0.40	0.42	0.80	0.70	0.99	0.47
ΣO (phenanthrenes/anthracenes)	1.97	0.93	1.26	2.70	3.17	1.65	1.84	0.79
Methylphen/phenanthrene	1.33	0.62	2.03	2.42	1.00	0.61	1.51	0.87
1,7diMePhen/2,6-diMePhen+1,7-diMePh	0.81	0.13	0.86	0.15	0.80	0.11	0.72	0.15
C2DBT/C2PH	0.18	0.15	0.98	2.72	0.77	0.93	2.11	3.24
C3DBT/C3PH	0.21	0.23	1.06	0.90	0.31	0.31	1.26	0.61
C2DBT/C2CRY	0.42	0.73	0.40	0.39	0.92	1.89	1.86	3.37
C3DBT/C3CRY	1.57	2.95	1.26	3.42	3.93	5.41	4.62	5.13
IP/(IP+BghiP)	0.49	0.09	0.45	0.26	0.50	0.15	0.43	0.25
ΣEPA 16PAH/Σalkylated PAH	0.20	0.08	0.13	0.07	0.20	0.07	0.15	0.05

None of the cores revealed ΣPAC trends similar to remote lakes in north-central North America, where maximum unsubstituted PAH deposition typically occurred during the mid-20th century and has declined toward modern times (see Table S3 in Kurek et al. 2013). Maximum concentrations and fluxes of unPACs from our study lakes were within the range typical of remote lakes, but substantially lower than lakes in urbanized catchments (Table S3 in Kurek et al.). For example, modern unPAC concentrations in the upper sediment intervals from three Albertan lakes within tens of kilometres of coal-fired power plants and extensive agricultural and residential developments (Donahue et al. 2006), were about one order of magnitude greater than maximum concentrations recorded by our study lakes, with the exception of NE20.

Metals: To facilitate comparison among our study lakes, we have grouped the lakes as near-field (NE13 and NE20; 0-20 km from AR6), mid-field (20-50 km from AR6), and far-field (>50 km from AR6) sites. In addition, due to the large number of metals considered, we focus our discussion first on five metals: aluminium (Al), calcium (Ca), vanadium (V), lead (Pb), and mercury (Hg), which represent the entire data set well. These elements uniquely characterize natural or anthropogenic sources in the region and they are spatially and temporally representative of patterns captured by the entire data set. For example, V is enriched (more than any other element) in bitumen from the AOSR (Jacobs and Filby, 1983, Hodgson 2006). Thus, as with previous studies (Shotyk et al. 2014), we rely on V as our primary geochemical tracer for oil sands extraction. We rely on Al to reconstruct changes in mineral (i.e., lithogenic) inputs, including the input of wind-blown dust. Pb and Hg are included because they are both released by various anthropogenic activities and have been shown to be higher in snow (Kelly et al. 2010; Kirk et al. 2014), lichen (Landis et al. 2012), and moss (Shotyk et al. 2014) collected close to the open pit mines (relative to samples collected further away). Finally, Ca is a key component of the carbonate terrain that underlies some of our study sites and the bitumen-bearing McMurray formation.

Exposure to contaminated sediments is a potential hazard to aquatic organisms. To assess the potential for this hazard, we first compared our lake sediment metal concentration data to existing sediment quality guidelines set by the Canadian Council of the Ministers of the Environment (CCME). Seven of the metals we measured (As, Cd, Cr, Cu, Pb, Hg, and Zn) have sediment quality guidelines set by the CCME. No exceedances of CCME guidelines for Cr, Cu, or Pb were observed; however, interim sediment quality guidelines (ISQG) were exceeded for As (in two lakes), Cd (in five lakes), Hg (in two lakes), and Zn (in three lakes), with the greatest number of exceedances occurring in L60 (Fig. 9). In addition, L60 and Gregoire Lake were the only lakes from which sediment intervals exceeded the probable effects levels (PEL; n=2 intervals in each lake).

To summarize spatial and temporal patterns among all 20 study lakes, we calculated 10-year mean trace element concentrations for near-field (<20 km from AR6), mid-field (20–50 km from AR6), and far-field (>50 km from AR6) sites. Our sediment cores are characterized by a high degree of spatial and temporal variability in trace element concentrations and fluxes (Fig. 9). For example, during the 18th and 19th centuries both V concentrations and fluxes were 2–3x higher and more variable in far-field sites than in near- or mid-field sites; however, after ~1960, V concentrations and fluxes in near-field sites increased rapidly, peaking at 30 μg/g and 8,000 μg/m^2/ y, respectively, during the 1980s. Near-field V concentrations and fluxes then decreased steadily, reaching near background levels in the most recent sediment intervals. Similar spatial and temporal patterns are evident for Pb, with two important differences: (i) Pb concentrations and fluxes remained highest in far-field sites throughout the past ~250 years; and (ii) Pb concentrations and fluxes increased contemporaneously and to a similar magnitude in both near- and mid-field sites. Hg concentrations and fluxes increased steadily over the past ~150 years in all lakes, with far-field sites exhibiting the highest Hg concentrations and fluxes. The range of Hg concentrations observed in our sediment cores (20–120 ng/g) are quantitatively similar to those reported by Neville et al. (2013) during their survey of surficial sediments from 63 lakes in the AOSR. Finally, Ca concentrations and fluxes are ~20x higher in near-field sites than in either mid- or far-field sites, while Al concentrations and fluxes remain higher in far-field sites than in all others. Neither Ca nor Al profiles exhibited a strong temporal trend, except for the variable Al concentrations in pre-1850 sediment.

Much of the variability in trace element concentrations and fluxes described above is removed after calculating EF and flux ratios (Fig. 10). For example, far-field V EF and flux ratios both remained stable (~1) for the past 250 years, in contrast to the high variability observed in V concentrations and fluxes in these lake systems. This suggests that V concentrations in these far-field lake systems are controlled by natural watershed inputs of lithogenic material. In contrast, V EFs and flux ratio profiles vary among near-and mid-field sites. For example, early increases in V flux ratios are noted during 1860s and 1920s in near-field sites, yet V EFs remained below two until the 1950. This

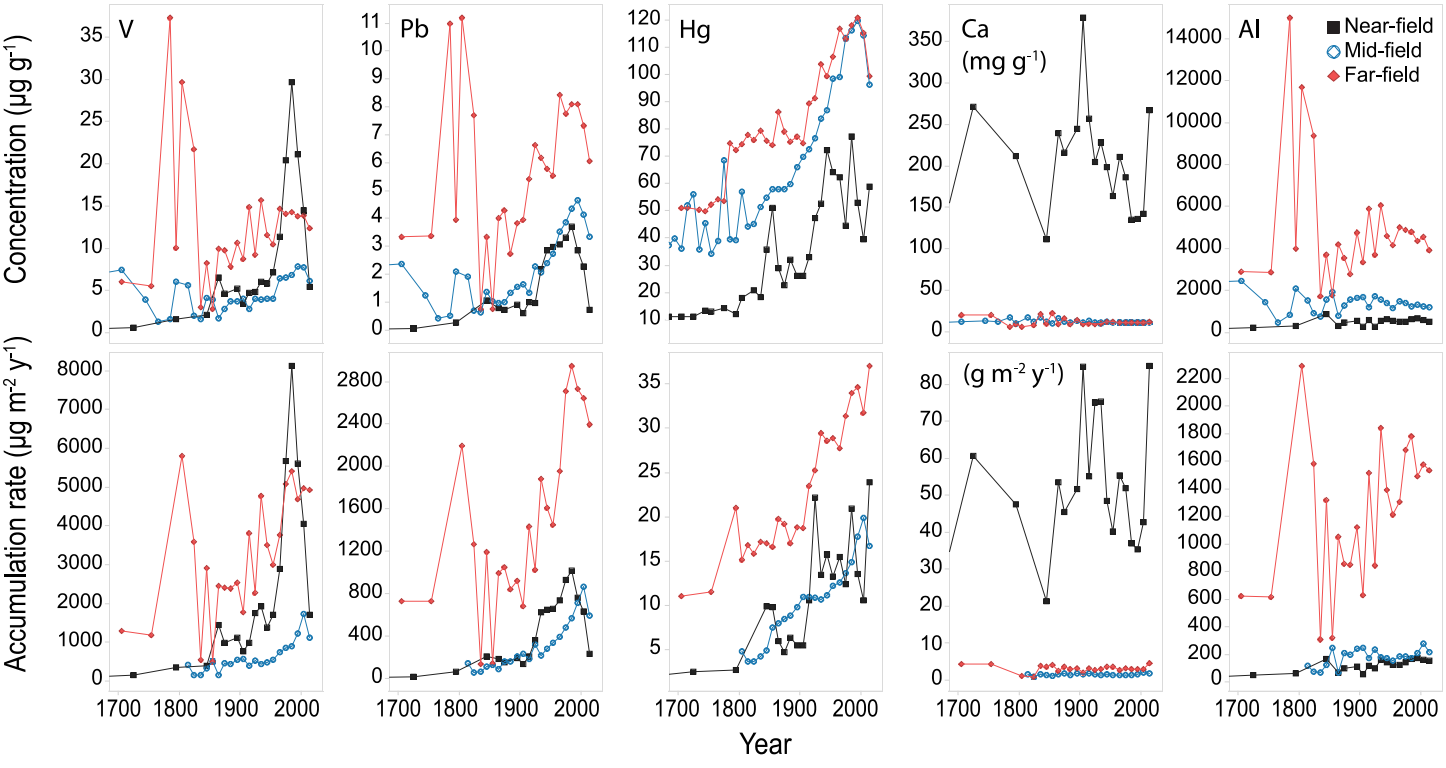

Figure 9. Elemental concentrations and fluxes for V, Pb, Ca, Hg, and Al within near-field (<20 km from AR6), mid-field (20–50 km from AR6), and far-field (>50 km from AR6) lakes. Note the different units for Ca.

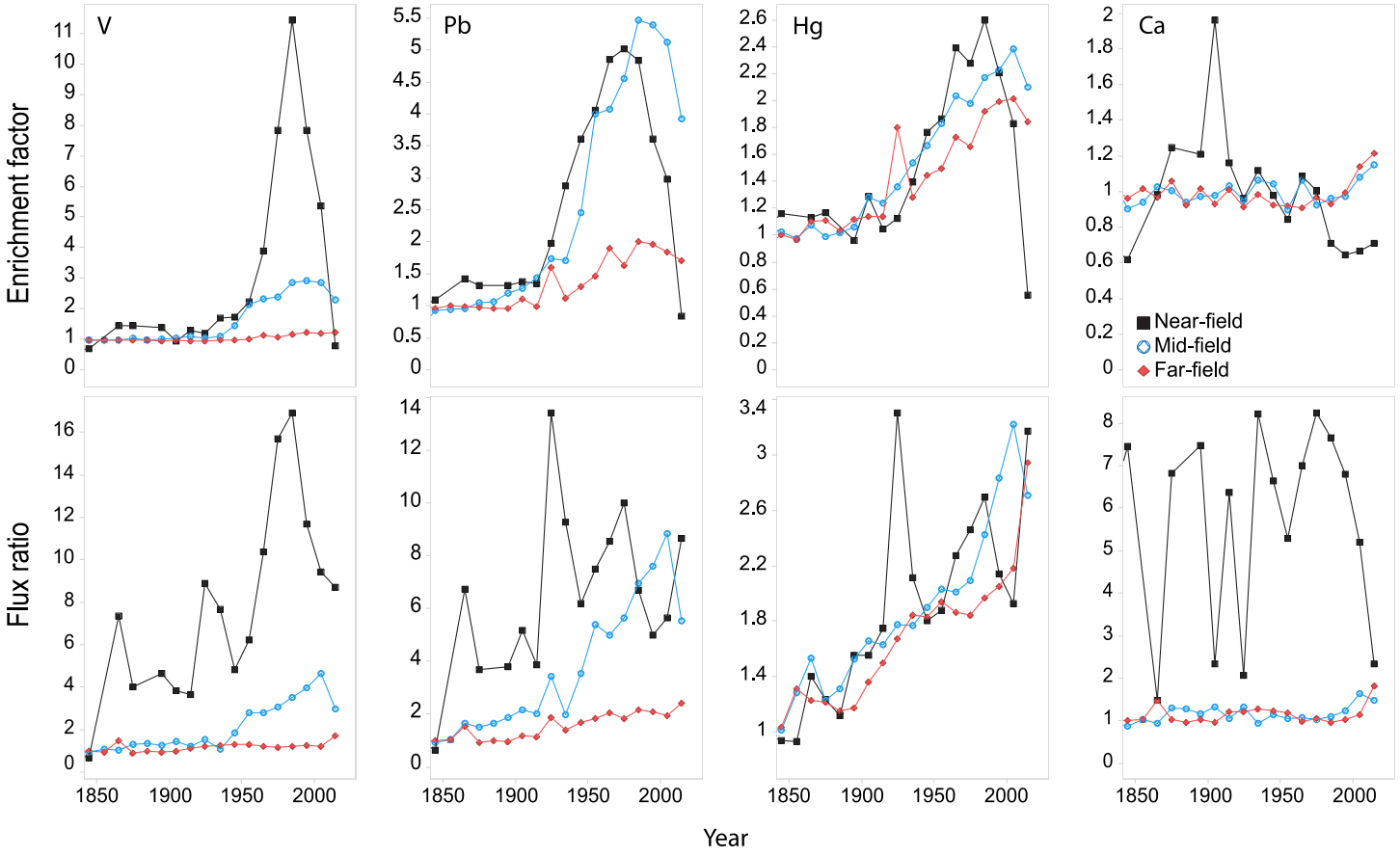

Figure 10. Profiles of 10-year mean enrichment factor (EF) and flux ratio for V, Pb, Hg and Ca. Lakes are grouped into near-field (n=2; black), mid-field (n=9; blue), or far-field (n=9; red).

discrepancy suggests pre-1950 increases in V flux ratios are likely due to an increase in lithogenic (i.e., mineral) matter, which increased sedimentation rates. In contrast, both V EFs and flux ratios increased rapidly in near-field sites after 1960, reaching 12 and 17x background, respectively, during the 1980s. Both ratios then decrease, though V EFs returned to one while V flux ratios remained elevated at ~9x background. A similarly timed (but smaller) increase is noted in V EF and flux ratios in mid-field sites, which rose to ~2x background after ~1950 before peaking at ~3x and 4x background, respectively, by 2000.

We attribute the rapid increase in V EF and flux ratios within near- and mid-field sites to the onset of regional oil sands extraction and processing, which were initiated in 1967 by Great Canadian Oil Sands (now Suncor). A second mine (Syncrude) opened in 1978, and, shortly after this time, we observe peak V EF and flux ratios in our near-field lakes (Fig. 10). While the size and extent of mining operations have continued to expand through time, our data suggest V loading to near-field sites has decreased steadily since the 1980s. This is despite a steady increase in mining operations through time. We suggest two possible explanations for this decrease in V delivery: changes in mining technology and emission control efforts. Initial mining operations relied upon use of long conveyor belts to move unprocessed bitumen from the mine to the extraction plant. The gradual replacement of these long conveyor belts during the 1980s and 1990s with heavy-haul trucks and shovels may have decreased fugitive dust emissions. Alternatively (or synergistically), installation of electrostatic precipitators on Suncor's upgrader stack in November 1979 may have also reduced particulate emissions. Support for this latter explanation comes from Landis et al. (2012), who characterized the trace element composition of various potential trace element sources, including stack emissions. They showed that particulate stack emissions averaged ~5x more V than any other source they measured. While the relative importance of each of these sources has likely changed through time, deposition of V to near-field lakes (i.e., those within

20 km of AR6) appears to have declined over the past three decades. In contrast, V deposition to sites located >20 km from AR6 steadily increased until the last decade. This is most likely a reflection of the steady expansion of mining activities across the landscape.

The Pb EF and flux ratio profiles exhibit a similar pattern to V (Fig. 10). For example, Pb flux ratios increased in near-field lakes during the 1860s and 1900s while Pb EFs were stable during this same period. However, unlike V, Pb EFs increased steadily in both near- and mid-field sites after ~1920, rising steadily to ~5 by the 1980s. A similarly timed, yet smaller, increase is also evident in far-field sites, in which Pb EFs rose to ~2x background over the same time period. Thus, both Pb EFs and flux ratios suggest greater Pb deposition to near- and mid-field sites than to far-field sites since the 1920s. This pattern suggests important sources of Pb beyond oil sands mining and processing. This is not surprising, as 20th century Pb pollution is a global phenomenon. Nonetheless, the higher Pb EFs and flux ratios in near- and mid-field sites (relative to far-field sites) strongly suggests enhanced Pb emissions associated with regional anthropogenic activities. These anthropogenic activities were very likely not limited to oil sands mining and processing, but possibly incorporate emissions from the city of Fort McMurray itself.

In contrast to V and Pb, Hg EF and flux ratios reveal remarkably similar profiles among all lakes, increasing steadily after ~1850 (Fig. 10). Both ratios rise to between two and three, and we observe little evidence for a significant increase after the onset of oil sands mining activities in 1967. Instead, our Hg records clearly record a 3-fold increase over the industrial era, which is consistent with other lake sediment cores recovered from across western North America (Drevnick et al. 2016) and around the globe (Biester et al. 2007, Engstrom et al. 2014). Thus, despite higher winter-time loadings of Hg close to the Suncor upgrader and associated petroleum coke piles (Kirk et al. 2014), we observe no obvious uptake in lake sediment Hg attributable to oil sands mining and processing.

Profiles of Ca EF and flux ratios exhibit a different temporal pattern than V, Pb, or Hg (Fig. 10). Near-field Ca EFs fluctuate through time, but remain below two. In contrast, Ca flux ratios range from 1 to 8, with considerable inter-decadal variability. There is little evidence for any increase in Ca delivery to mid- or far-field sites, as Ca EFs and flux ratios both remain below two throughout the period of record. This is despite evidence from spatial surveys of lichens (Landis et al. 2012), wet atmospheric deposition (Lynam et al. 2015), and regional soils (Fenn et al. 2014; Watmough et al., 2014, Wang et al., 2015) all of which reveal high inputs of base cation deposition at sites located close to modern-day mining operations. The source of these base cations is fugitive dust, which is emitted to the atmosphere from a wide range of sources. Source receptor modeling which compared metal signatures among potential atmospheric emission sources and lichen collected in 2008 suggests that important emissions sources of fugitives dust to the oil sands region are: oil sand and processed material (~11-15%), tailing sand fugitive dust (~19-25%), combustion processes (~19-23%), limestone and haul road fugitive dust (~15-17%), and a general urban source (~15%) (Landis et al. 2012). Indeed, atmospheric base cation deposition has been shown to mitigate the risk of soil acidification from NO_x and SO_2 emissions (Fenn et al. 2014; Watmough et al. 2014). In contrast, our sediment cores suggest fugitive dust emissions have yet to measurably change regional lake sediment Ca concentrations.

Considered collectively, our results indicate that normalization to a conservative lithogenic element (in our case Al) provides evidence for changes in sources of trace element emissions through time. This supports the recent suggestion of Wiklund et al. (2014) that this approach be used to identify trace element pollution in regional freshwater systems. Our results also demonstrate that EFs have not been stable through time; near-field V EFs first increased to ~12 during the l980s, but they have returned to ~1 over the past ~20 years. This is despite a rapid expansion in the number and size of mines over this same period. We suggest this reflects a shift in the predominant source of atmospheric trace element emissions through time. During early mining and upgrading operations, which were limited to Suncor and Syncrude, blowing dust from the use of conveyor belts and stack emissions were likely the two most important sources of anthropogenic V emissions to the atmosphere. But improvements to mining tech-

nology and an increase in the aerial extent of open-pit mines appears to have changed the relative importance of different sources within the region. Today, fugitive dust emissions have many different sources, including haul road dust, overburden, processed materials (e.g., coke), tailing sands, and fleet emissions. This is why, for example, Shotyk et al. (2014) report a near linear relationship between the concentration of Pb and various lithogenic elements in living moss. Our lake sediment core results place these recent findings in a long-term context, and help to mitigate the lack of consistent environmental monitoring over the past ~40 years of anthropogenic activities within the Athabasca Oil Sand region.

Principal components analysis: The results summarized above for just a few elements reveal large spatial differences in the geochemical composition of regional lake sediments. Nonetheless, these results are broadly representative of our entire geochemical data set, as illustrated by the PCA results (Fig. 11). The first axis (PC1; λ=59 %) is dominated by positive loadings of all elements measured except for Na, Sr, and Ca. The second axis (PC2; λ=10 %) is dominated by high positive loadings for Ca, Sr, and Mg and negative loadings for Hg, Cd, and Zn. This pattern reflects the much higher trace element concentrations in two of our far-field sites (Gregoire Lake and L60) and the ~20x higher base cation concentrations in our two near-field study sites (NE13 and NE20). In addition, we see almost complete separation of our study sites based upon their PC sample scores, with little overlap among near-, mid-, and far-field sample scores.

The PCA results summarized above suggest the geochemical differences among our study sites are controlled by each lake's location on the landscape. The highest concentrations of nearly every element measured are found in sites located >50 km from AR6 (Fig. 6). Similar spatial variability is also evident in the results of an annual water quality monitoring survey of 50 regional lakes. Lakes located in the Birch Mountains (including L60) are characterized by trace metal concentrations that are elevated relative to lakes located closer to the open pit mines. The Birch Mountains host metal-rich black shales that in some cases approach economically significant concentrations (Dufresne et al. 2001). Thus, we suggest the high metal concentrations observed within our three Birch Mountain lake sediment cores (Lakes L60, 2014-X, and 2014-Z) are reflective of their unique bedrock geology, and are not due to anthropogenic impact. In contrast, two of our study sites (Gregoire Lake and Pushup Lake) rest within watersheds affected by anthropogenic activities. This likely accounts for the higher trace element concentrations noted in these two lake systems.

The much higher trace element concentrations noted in the far-field Gregoire Lake and L60 mask any other variability among our study sites; therefore, we removed these two lakes and reran the PCA (Fig. 11). Ca, Sr, and Mg still load negatively along PC1, and we now observe a greater range of species and sample scores. We also observe greater variability among lakes than within any individual lake, with sites located closer to AR6 exhibiting higher concentrations of Ca, Sr, and Mg, and therefore lower PC1 and higher PC2 sample scores. However, this spatial pattern cannot be due to deposition of atmospheric oil sands emissions. If this were the case, we would expect a shift from positive to negative PC1 sample scores after the onset of oil sands extraction activities (i.e., after 1967). Instead, we hypothesize that the input of carbonate-rich groundwater drives this spatial pattern. Lakes NE13 and NE20 rest near surficial outcrops of the carbonate-rich Waterways Formation and the bitumen-bearing McMurray Formation. Groundwater within both formations can be highly saline because of the dissolution of halite and anhydrite-containing evaporite units (Cowie et al. 2015). Indeed, high-salinity groundwater discharges directly to the Athabasca River (Gibson et al. 2013). Thus, we suggest that regional geology, and not the open-pit mines, drive the overall geochemical composition of lake sediments within the Athabasca Oil Sands region.

Climate-induced changes to lake limnology: VRS chl *a* analyzes show that modern inferred primary production is greater than background values at all 23 sites analyzed, regardless of proximity to industry (Fig. 12). Most sites demonstrate relatively stable background (generally pre-1970s) VRS-chl *a* concentrations followed by abrupt increases. Unlike the other sites, RAMP 175 shows a decreasing VRS-chl *a* trend beginning ~2005. Similarly, RAMP 226

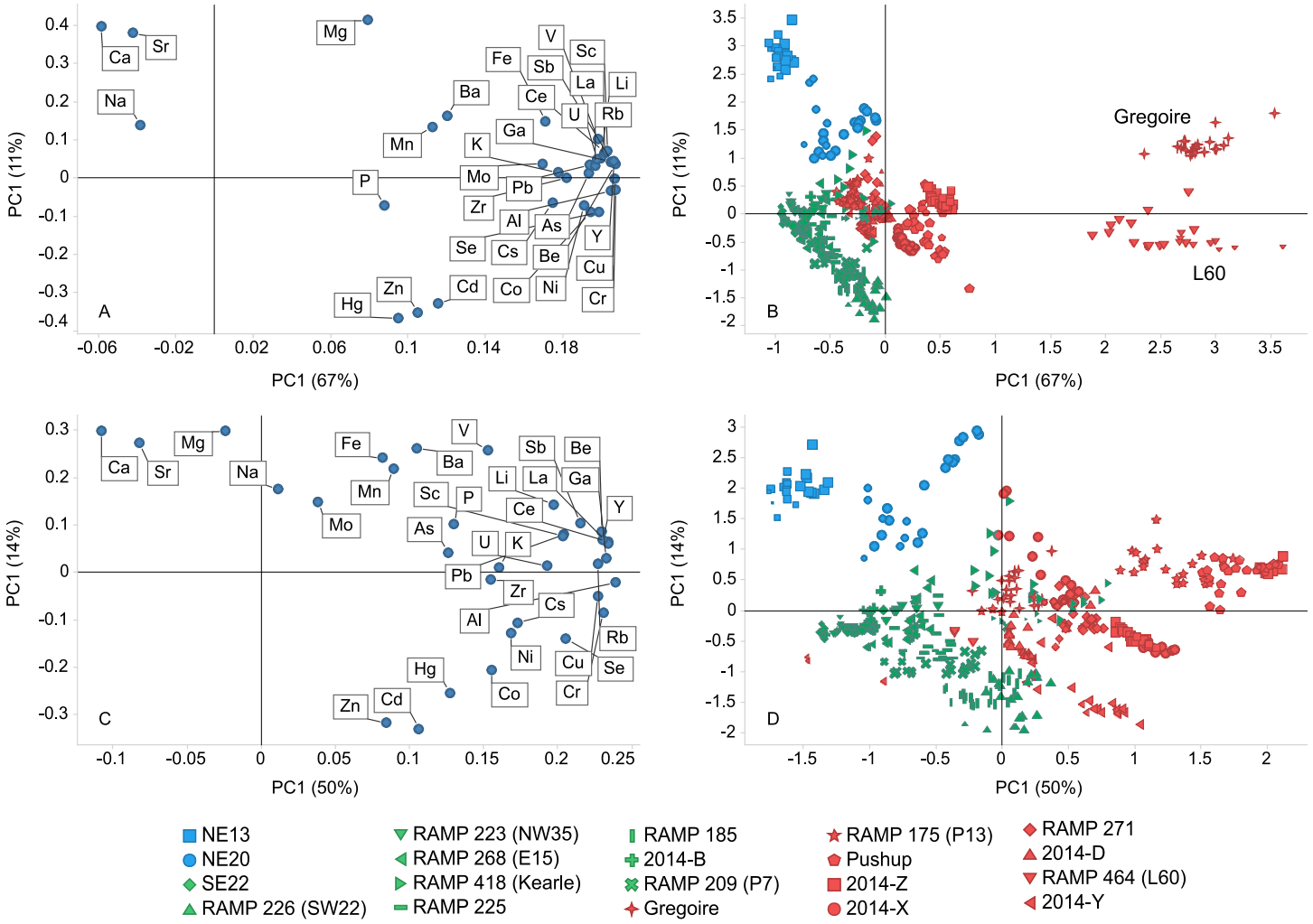

Figure 11. Results of the Principal Component Analysis (PCA). Panels A and B include all lake sediment cores, while panels C and D contain results of a second PCA run after excluding Gregoire and L60. Sample scores are sized according to sample age, with older samples appearing as smaller symbols and are coloured according near-field (n=2; green), mid-field (n=9; blue), or far-field (n=9; red).

shows a decreasing trend from the late 1990s to the late 2000s with a subsequent return to early 1990s concentrations by 2011. Pushup Lake also shows a slight decrease in VRS-chl *a* from the late 1990s to the mid-2000s. Although VRS-chl *a* profiles from these lakes differ from the regional patterns of consistent primary production increases, modern VRS-chl *a* values are still higher than the pre-oil sands development values at these three sites, resulting in enrichment factors >1. VRS-chl *a* enrichment factors were >1 at all 23 sites, averaging 1.8 (range 1.1 to 5.3). Breakpoint analyzes on VRS-chl *a* concentrations from each lake identified abrupt changes ranging from ~1919 to ~2006, with 83 % (15 out of 18) of the lakes on which breakpoint analyzes were performed changing abruptly at ~1970 or later.

An assessment of Cladoceran fossil remains in the five 2011 study lakes shows shifts in the cladoceran assemblages during the ~1960-1970s for all sites except SW22, where the shift occurred at ~1900 (Fig. 14; Kurek et al. 2012). Daphniids increased as a percentage of the cladoceran assemblage between the mid-1900s and modern times at all sites (Fig. 14), despite the low quantity of pelagic habitat in these shallow lakes. Magnitudes of the daphniid increase varied depending on the dominance of Bosmina, Alona, and/or Chydorus in each sediment record. NE20 showed by far the largest daphniid increase beginning at ~1970. At NE13 and SE22, daphniids became more frequent and abundant in the most recent assemblage zone, delineated at ~1960. Daphniids never exceeded ~4 % and 8 % abundance at NE13 and SE22,

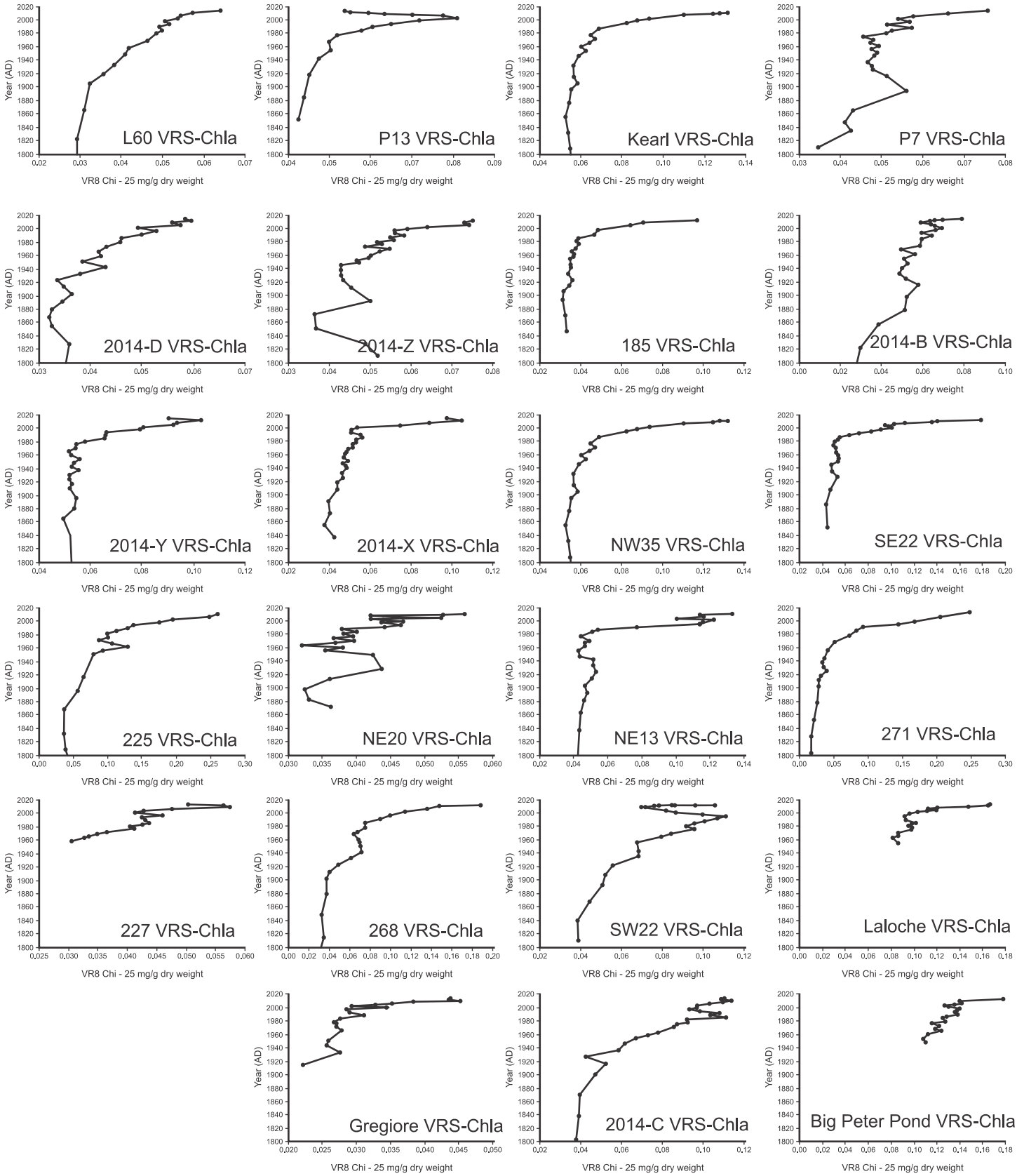

Figure 12. VRS Chl *a* profiles from 1800 to modern times for all 23 study sites. Profiles are approximately arranged according to geographic location or distance from the centre of the major oil sands developments.

respectively. At the western sites, daphniids increased in abundance in the post mid-1900s sediments. Between the mid-1900s and modern times, daphniids tripled and doubled their average abundance at NW35 and SW22, respectively, although, abundances remained low. These results suggest that the sentinel zooplankton *Daphnia* has not yet been affected negatively by decades of high atmospheric PACs and metals deposition (Kurek et al. 2012).

Pearson correlation analyzes identified significant ($p<0.05$) positive correlations between mean annual and seasonal air temperatures and VRS-chl *a* Z scores in all the lakes. No significant correlations were identified between VRS-chl *a* and mean annual and seasonal precipitation. These findings suggest climate warming as a likely driver of increased aquatic primary production in the oil sands region. Both average annual and seasonal air temperatures are increasing in the oil sands region (Fig. 13), which could facilitate favourable conditions for primary producers. Specifically, the correlations between VRS-chl *a* and increased temperatures in the winter, spring, and fall suggest a longer growing season for primary producers as one likely mechanism. Lake ice phenology and

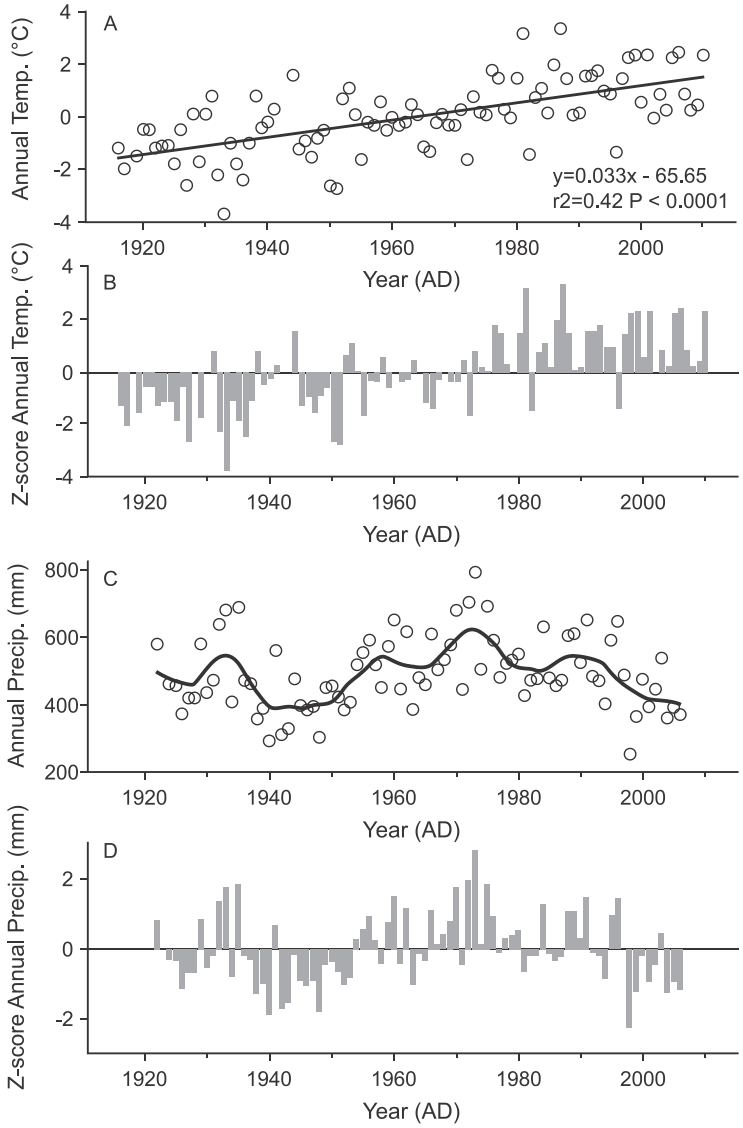

Figure 13. Annual temperature (1916-2010 AD) and precipitation (1922-2006 AD) observations from Fort McMurray, Alberta. A linear regression describes the annual temperature trend (A). A locally-weighted regression with a span of 0.15 highlights the precipitation trends (C). Standardized values (Z-scores) were calculated to emphasize the annual variability of temperature (B) and precipitation (D) compared to the long-term means of each record. Historic climate data from the Fort McMurray station (#3062696) were provided by the Government of Canada's Adjusted and Homogenized Canadian Climate Data website (www.ec.gc.ca/dccha-ahccd/).

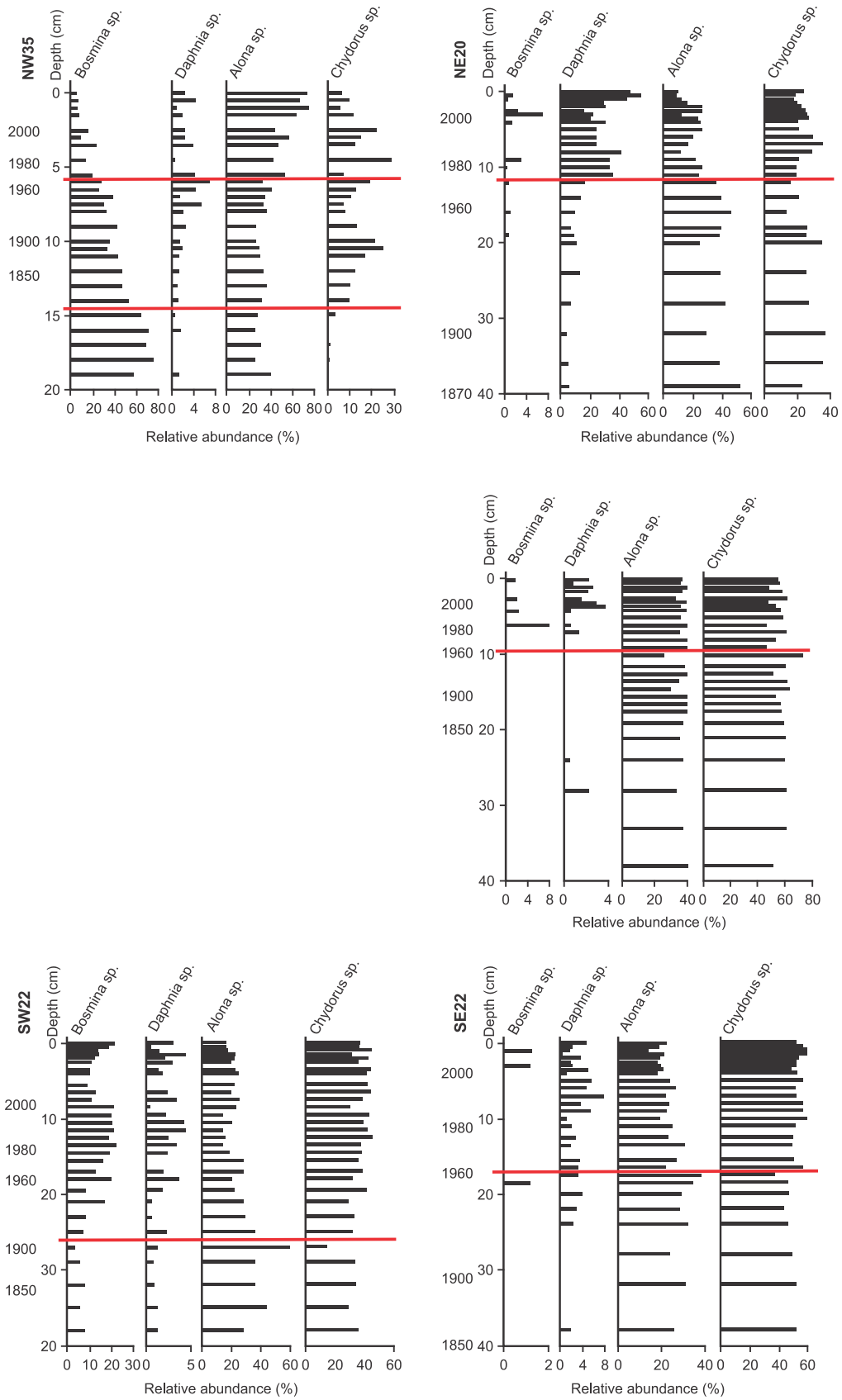

Figure 14. Stratigraphies of cladoceran assemblages from the five study lakes proximate to the major oil sands development plotted against core depth. Select dates from each core are also provided. *Bosmina* and *Daphnia* were the principal pelagic taxa. *Chydorus* and groupings of two to four *Alona* species represented the dominant substrate-affiliated taxa. Minor contributors to the assemblages were not plotted, but were used to calculate relative abundances. The horizontal lines (red) represent cladoceran assemblage zone boundaries defined by constrained clustering and the broken-stick model.

stability of the water column are some of the most important controls on primary production and aquatic biological communities in ice-covered lakes (Smol et al. 2007, Rüland et al. 2013, Rüland et al. 2015) and favourable shifts in light conditions and nutrient availability that accompany an earlier ice-off period are known to stimulate primary production (Weyhmeyer et al. 2001).

3.3 Summary and Conclusions

Analysis of dated lake sediment cores collected from lakes located 10-200 km from the major developments shows that atmospheric deposition of PACs and inorganic contaminants, including metals V, Pb, and Hg has increased since oil sands development began in this region in the 1960s with impacts most pronounced in near- and mid-field lakes (<50 km from the major development). Examination of diagnostic PACs ratios indicated that recent (post-2000) sediment horizons showed evidence of greater petrogenic influence than those from before Oil Sands development began (pre-1960s). Comparison of metals concentration data to CCME sediment quality guidelines demonstrated that the ISQG was exceeded for As (in two lakes), Cd (in five lakes), Hg (in two lakes), and Zn (in three lakes) while the PEL guideline was exceeded for As in only two sediment intervals in two study lakes. Results from PCA analyzes suggest that regional bedrock (i.e., McMurray and Waterways formations, Birch Mountains) exerts a first-order control over the broad geochemical composition of lake sediments. Despite the influence of bedrock geology on metals concentrations and fluxes in this region, we were able to detect metals enrichment beginning in the 1960s and attributable to oil sands development, including increasing V/Al ratios and V fluxes.

VRS chl *a* analyzes demonstrate that modern inferred primary production is greater than background values at all 23 sites analyzed, regardless of proximity to industry. Significant ($p<0.05$) positive correlations were found between mean annual and seasonal air temperatures and VRS-chl *a* Z scores in all the lakes suggesting that climate warming is a driver of increased aquatic primary production in the oil sands region. Assessment of Cladoceran fossil remains in five study lakes shows post-1960-70s (post-1900s in SW22) shifts in the cladoceran assemblages. Daphniids increased as a percentage of the cladoceran assemblage between the mid-1900s and modern times at all sites, suggesting that the sentinel zooplankton *Daphnia* has not yet been negatively impacted by decades of high atmospheric PACs and metals deposition. Our findings of changes in lake primary productivity and cladoceran fossil remains over the past ~100 years suggest that lake ecosystems have entered new ecological states distinct from those of previous centuries. The dated lake sediment core study presented here was designed to be integrated with other JOSM components. For example, PACs and metals analyte lists for sediment measurements were the same as for the water quality, air, invertebrate, fish and wildlife monitoring programs.

Box 1. Case Study – Mercury in the Oil Sands Region

Mercury (Hg) is a global pollutant of concern, primarily because methyl mercury, a potent neurotoxin, can bioaccumulate and biomagnify through food webs, reaching levels in top predators that may pose health risks to people consuming them. In the Athabasca Oil Sands region, there are Hg consumption advisories for Athabasca River walleye downstream of Fort McMurray as well as a gull and tern egg consumption advisory in the Peace Athabasca Delta, located ~200 km from major oil sands developments.

Often, it is difficult to determine why MeHg in biota is high in some regions and not in others because the cycling of Hg in the environment is complex. Different forms of Hg are present in the environment, each one of which can undergo various environmental transformations. Gaseous Hg(0) is the form of Hg primarily released to the environment from anthropogenic sources, such as coal burning. Because Hg(0) can undergo long-range transport, both local and distant sources contribute to atmospheric deposition of inorganic Hg(II), which is produced by atmospheric oxidation of Hg(0) and is rapidly deposited to landscapes and water bodies in wet and dry deposition. Once in aquatic ecosystems, such as lakes and wetlands, inorganic Hg(II) can be methylated to MeHg by naturally occurring microbes, such as sulphate reducing bacteria. The newly produced MeHg can then be taken up by organisms. Hg(II) and MeHg may be also emitted directly to the atmosphere from local point sources and then deposited to nearby ecosystems.

In this study, we used snowpack measurements and dated lake sediment cores to determine spatial and temporal trends in Hg deposition to the Athabasca Oil Sands region. The snow pack represents a temporally integrated measure of atmospheric deposition spanning the time period between first snowfall to sampling; therefore, sampling of the spring-time accumulated snow pack at numerous sites across the landscape provides a measure of net ecosystem THg and MeHg loads to the sampling region. Measurement of springtime snowpack loadings at 90 sites located within 200 km of the major development area showed that total Hg (THg; all forms of Hg in a sample) and MeHg loadings were elevated at many sites near the major development area, reaching up to 1,420 and 19 ng/m^2, respectively, with areas of maximum THg and MeHg loadings located between the Muskeg and Steepbank rivers and resembling a bullseye pattern on the landscape. Loadings decreased rapidly with distance from the major developments and reached background in the Peace Athabasca Delta located ~200 km from the major development area.

In the absence of long-term monitoring in the oil sands region, analyzes of dated lake sediment cores provide a way to determine changes in Hg deposition since oil sands development began and to compare current deposition patterns to natural variation in the region. Analyzes of dated sediment cores collected from lakes located 10-100 km from the major development area showed that Hg deposition began increasing in this region first in the early 1900s, reflecting increasing national and global Hg emissions. Analyzes of additional snowpack and sediment core data are on-going, as is integration with data from JOSM programs on air, water, and biota. For example, snowpack Hg measurements are currently being used to ground-truth Hg deposition models for the region. Integration with water and biological monitoring will allow us to quantify the impacts of atmospheric THg and MeHg deposition on Athabasca River and tributary water, invertebrate, and fish Hg concentrations.

4. Atmospheric Theme Assessment with Future Research Needs and Recommendations

Analyzes of snowpack and lake sediment core data collected over 2011-2014 show that deposition of contaminants, including PACs and a variety of metals including Hg and MeHg, is most elevated close to the major developments and remains above background for 50-75 km from them. These findings agree with those with other multi-media measurements including air (Harner et al. 2013) as well as lichen measurements carried out by the Wood Buffalo Environmental Association (WBEA) (Graney et al. 2012), although detailed comparisons of these various measurements as well as year-round precipitation measurements are currently underway. Results from these same multi-media measurements also indicate that fugitive dusts (e.g., mining, tailings, on/off roads, etc.) are important contributors to contaminant deposition in the Athabasca Oil Sands region (Kirk et al. 2014, Manzano et al. 2016, Graney et al. 2012, Landis et al. 2012). Results of snowpack (Kirk et al. 2014, Manzano et al. 2016), sediment core (Kurek et al. 2013, Cooke et al. in preparation), PACs air sampling (Harner et al. 2013), and lichen sampling (Graney et al. 2012) all agree that atmospheric contaminant deposition is close to background beyond ~50-75 km. Analysis of proxies, such as dated lake sediment cores, provides the only way to assess pre-development conditions and the variation in background conditions in this region. Analyzes of numerous dated lake sediment cores collected 10-200 km from the major developments show that atmospheric deposition of PACs and numerous inorganic contaminants has increased since oil sands development began in this region in the 1960s. Analysis of VRS-chl *a* and invertebrate fossil remains in these same lake sediment cores reveals that lake primary productivity has increased and invertebrate communities have changed over the past ~100 years. Our paleolimnological work on the health of algal and invertebrate communities in oil sands region lakes adds significantly to limited data in this area. As such it is recommended that this work should be continued in conjunction with analyzes of the novel markers described below.

The JOSM program, *Atmospheric deposition to the Athabasca Oil Sands region using snowpack measurements and dated lake sediment cores* was designed so that data can be integrated with the water quality, air, invertebrate, fish and wildlife monitoring programs. For example, snowpack samples were collected at air, invertebrate and fish and wildlife monitoring sites so that contaminant loads at these different monitoring sites can be provided to various program partners. Sampling was conducted so that catchment scale contaminant deposition can be determined for the Steepbank, Muskeg and Ells rivers, where integrated focused studies are being carried out. In some cases, integration is already underway. For example, snowpack sample dissolved and particulate-bound THg loadings are currently being used to ground-truth atmospheric Hg deposition models. To integrate atmospheric deposition measurements with water quality measurements to determine how aerial deposition to the landscape affects water quality in the tributaries and Athabasca main stem, additional modelling that incorporates regional hydrology is needed.

Results presented here indicate several priority needs for future monitoring and research. Comparison of snowpack PACs data from 2009-2014 with those reported by Kelly et al. (2009) for 2008 showed no clear temporal trend in snowpack loadings to the landscape from 2008 and 2011-2014, suggesting that additional snowpack monitoring is needed. We recommend annual snowpack sampling be conducted at a subset of sites (n=~40) located varying distances from the major developments and in the Peace Athabasca Delta to track short-term temporal trends in contaminant deposition and changes in background conditions. A large-scale survey (n=~140 sites) at sites located across a grid-work pattern on the landscape should be carried out every ~2-3 years to determine net spring-time contaminant loadings to the lower Athabasca River and its tributaries, and to examine changes in spatial depositional patterns as oil sands developments change. Some contaminants, such as THg and MeHg, can undergo post-depositional processing in snow packs. We recommend targeted research projects to quantify production and losses of key contaminants of concern in snow packs, such as production of MeHg via methylation in snow or snow melt and losses of THg and MeHg via photoreduction and photodemethyaltion, respectively.

Results from the snowpack and lake sediment core program, and also from air and precipitation monitoring, suggest that analysis of source materials, including road haul materials, dusts emitted from open pit mines, upgrader facility stack emissions, and tailings pond material for PACs and metals is needed to determine the relative importance of various emission sources to contaminant deposition. Analyzes of these source materials, combined with identification of novel industrial and/or natural sourced markers in the receiving environment (i.e., air, water, snow, and sediment), will allow quantification of the relative importance of various industrial and natural processes to contaminant deposition. Promising tools that should be applied to environmental measurements, such as snow and sediment cores, include measurement of black carbon particles, use of two- dimensional gas chromatograph time of flight mass spectrometry (2DGC-TOF-MS) to more fully characterize PACs in the receiving environment, and analyzes of natural abundance compound specific radiocarbon (CSRA; for PACs) (Jauzy et al., 2013) and stable isotopes (for Hg) (Blum et al., 2012). Some of these analytical techniques could also be applied to biota, such as invertebrates and fish, to track the bioaccumulation of industrial and natural sourced contaminants into aquatic and terrestrial food webs. Finally, results from multi-media analyzes demonstrate that more complete information on emissions, especially fugitive sources, are needed to reconcile emissions with environmental measurements and to accurately model atmospheric contaminant transport, transformation and deposition.

5. Acknowledgements

Developing snow field sampling protocols and sampling designs: Sunny Cho, Rod Hazewinkel, Shelley Manchur (AESRD). Snow sampling design and snow collections in the Peace Athabasca Delta 2012-2015: Bruce Maclean (Mikisew Cree First Nation), Jason Straka (Parks Canada) and residents of Fort Chipewyan. Field and Laboratory Support: Richard Frank, Xiaowa Wang, Amy Sett, Meagan Rodrigues, Jessica Power, Catherine Wong, Jenelle Backer, Moriah Tanguay, Jonathan Keating, Technical Operations and Scientific Presentation and Design Support Services at the Canada Centre for Inland Waters, Burlington, Wood Buffalo Helicopters.

6. Literature Cited

AMAP (2011) AMAP Assessment 2011: Mercury in the Arctic. Arctic Monitoring and Assessment Programme. Oslo, Norway, pp 193

Amyot M, Lean DRS, Poissant L, Doyon MR (2000) Distribution and transformation of elemental mercury in the St. Lawrence River and Lake Ontario. Can J Fish Aquat Sci 57:155-163

Appleby PG (2001) Chronostratigraphic techniques in recent sediments. In: Last WM, Smol JP (eds) Tracking Environmental Changes Using Lake Sediments, vol 1. Kluwer Academic Publishers, Dordrecht, Netherlands, pp 171-203

Arellano L et al (2014) Persistent organic pollutant accumulation in seasonal snow along an altitudinal gradient in the Tyrolean Alps. Environ Sci Pollut Res 21:12638-12650

Barkay T, Niels K, Poulain AJ (2011) Some like it cold: microbial transformations of mercury in polar regions. Polar Res 30. doi: 10.3402/polar.v30i0.15469

Benoit JM, Gilmour CC, Heyes A, Mason RP, Miller CL (2003) Geochemical and biological controls over methylmercury production and degradation in aquatic ecosystems. In: Chai Y, Braids OC (eds) Biogeochemistry of Environmentally Important Trace Elements. American Chemical Society, Washington, D.C., p 262-297

Blais JM, Donahue WF. Comment on "Sphagnum mosses from 21 ombrotrophic bogs in the Athabasca bituminous sands region show no significant atmospheric contamination of 'heavy metals'". Environ Sci Technol 49: 6352-3.

Blanchard P et al (2005) Atmospheric Deposition of Toxic Substances to the Great Lakes: IADN Results through 2005. Environment Canada and the United States Environmental Protection Agency, pp 223

Bloom NS, Crecelius EA (1983) Determination of mercury in seawater at subnanogram per liter levels. Mar Chem 14:49-59

Bloom NS (1989) Determination of picogram levels of methylmercury by aqueous phase ethylation, followed by cryogenic gas chromatography with cold vapour atomic flourescence detection. Can J Fish Aquat Sci 46:1131-1140

Blum JD, Johnson MW, Gleason JD, Demers JD, Landis MS, Krupa S (2012) Mercury concentration and isotopic composition of epiphytic tree lichens in the Athabasca oil sands region. In: Percy KE (ed) Alberta Oil Sands: Energy, Industry and the Environment. Elsevier, Kidlington, Oxford, p 373-390

Boës X, Rydberg J, Martinez-Cortizas A, Bindler R, Renberg I (2011) Evaluation of conservative lithogenic elements (Ti, Zr, Al, and Rb) to study anthropogenic element enrichments in lake sediments. J Paleolimnol 46:75-87

Boutron CF, Candelone JP, Hong S (1995) Greenland snow and ice cores: unique archives of large-scale pollution of the troposphere of the Northern Hemisphere by lead and other heavy metals. Sci Total Environ 160-161:233-241

Brooks S, Arimoto R, Lindberg S, Southworth G (2008) Antarctic polar plateau snow surface conversion of deposited oxidized mercury to gaseous elemental mercury with fractional long-term burial. Atmos Environ 42:2877-2884

Canadian Council of Ministers of the Environment (CCME) (2014) http://st-ts.ccme.ca/. Accessed January 2014.

Cho S, Sharma K, Brassard B, Hazewinkel R (2014) Polycyclic Aromatic Hydrocarbon Deposition in the Snowpack of the Athabasca Oil Sands Region of Alberta, Canada. Water Air Soil Pollut 225:1-16

Cooke CA, Bindler R (2015) Lake Sediment Records of Preindustrial Metal Pollution. In: Blais JM, Rosen MR, Smol JP (eds) Environmental Contaminants. Developments in Paleoenvironmental Research. Springer, Netherlands, p 101-119

Cowie BR, James B, Mayer B (2015) Distribution of total dissolved solids in McMurray Formation water in the Athabasca Oil Sands Region, Alberta, Canada: Implications for regional hydrogeology and resource development. AAPG Bulletin 99(1):77-90

Constant P, Poissant L, Villemur R, Yumvihoze E, Lean D (2007) Fate of inorganic mercury and methyl mercury within the snow cover in the low arctic tundra on the shore of Hudson Bay (Québec, Canada). J Geophys Res Atmos (1984–2012) 112. doi:10.1029/2006JD007961

Dittman JA, Shanley JB, Driscoll CT, Aiken GR, Chalmers AT, Towse JE, Selvendiran P (2010) Mercury dynamics in relation to dissolved organic carbon concentration and quality during high flow events in three northeastern US streams. Water Resource Res 46:1-15

Dodson SI, Frey DG (2001) Cladocera and other branchiopoda. In: Thorpe JH, Covich AP (eds) Ecology and Classification of North American Freshwater Invertebrates. Academic Press, New York, p 849-913

Driscoll CT, Yan C, Schofield CL, Munson R, Holsapple J (1994) The mercury cycle and fish in Adirondack lakes. Environ Sci Technol 28:136-143

Driscoll CT, Mason RP, Chan HM, Jacob D, Pirrone N (2013) Mercury as a global pollutant: sources, pathways, and effects. Environ Sci Technol 47:4967-4983

Durnford D, Dastoor A, Figueras-Nieto D, Ryjkov A (2010) Long range transport of mercury to the Arctic and across Canada. Atmos Chem Phys Disc 10:4673-4717

Durnford D, Dastoor A (2011) The behavior of mercury in the cryosphere: a review of what we know from observations. J Geophys Res 116. doi:10.1029/2010JD014809

Durnford D, Dastoor A, Ryzhkov A, Poissant L, Pilote M, Figueras-Nieto D (2012) How relevant is the deposition of mercury onto snowpacks? Part 2: A modeling study. Atmos Chem Phys 19: 9251-9274

Dufresne MB, Eccles DR, Leckie DA (2001) The geological and geochemical setting of the Mid-Cretaceous Shaftesbury Formation and other Colorado Group sedimentary units in Northern Alberta 9. Alberta Energy and Utilities Board, Alberta Geological Survey, pp 47

Environment Canada (2013) AAQS/AQRD Analytical Method for the Determination of Selected PACs in Ambient Air Samples-Method 3.03/5.1/M. Ottawa, Ontario, pp 27

Evans M, Talbot A (2012) Investigations of mercury concentrations in walleye and other fish in the Athabasca River ecosystem with increasing oil sands developments. J Environ Monit 14: 1989-2003

Gilmour CC, Henry EA, Mitchell R (1992) Sulfate stimulation of mercury methylation in fresh-water sediments. Environ Sci Technol 26:2281-2287

Graney JR, Landis MS, Krupa S (2012) Coupling lead Isotopes and element concentrations in epiphytic lichens to track sources of air emissions in the Athabasca oil sands region. In: Percy K E (ed) Alberta Oil Sands: Energy, Industry and the Environment. Elsevier, Kidlington, Oxford, p 343-372

Graydon JA, St. Louis VL, Hintelmann H, Lindberg SE, Sandilands KA, Rudd JW, Kelly CA, Hall BD, Mowat LD (2008) Long-term wet and dry deposition of total and methyl mercury in the remote boreal ecoregion of Canada. Environ Sci Technol 42:8345-8351

Gobeil C, Tessier A, Couture RM (2013) Upper Mississippi Pb as a mid-1800s chronostratigraphic marker in sediments from seasonally anoxic lakes in Eastern Canada. Geochim Cosmochim Acta 113:125-135

Hazewinkel RRO, Wolfe AP, Pla S, Curtis C, Hadley K (2008) Have atmospheric emissions from the Athabasca Oil Sands impacted lakes in northeastern Alberta, Canada? Can J Fisheries Aquat Sci 65:1554-1567

Hodgson GW (2006) Vanadium, nickel, and iron trace metals in crude oils of Western Canada. AAPG Datapages/Archives, p 1-18

Hammerschmidt CR, Lamborg CG, Fitzgerald WF (2007) Aqueous phase methylation as a potential source of methylmercury in wet deposition. Atmos Environ 41:1663-1668

Harner T, Su, K, Genualdi S, Karpowic J, Ahren L, Mihele C, Schuster J, Charland JP, Narayan J (2013) Calibration and application of PUF disk passive air samplers for tracking polycyclic aromatic compounds (PACs). Atmos Environ 75: 123-128.

Hintelman, H (2010) Organomercurials: their formation and pathways in the environment. Met Ions Life Sci 7:365-401

Horvat M, Bloom NS, Liang L (1993) Comparison of distillation with other current isolation methods for the determination of methyl mercury compounds in low level environmental samples. Part II. Water Anal Chim Acta 281:135-152

Jacobs F, Filby R (1983) Solvent extraction of oil-sand components for determination of trace elements by neutron activation analysis. Anal Chem 55(1):74-77

Jautzy J, Ahad JME, Gobeil C, Savard MM (2013) Century-long source apportionment of PAHs in Athabasca oil sands region lakes using diagnostic ratios and compound-specific carbon isotope signatures. Environ Sci Technol 47:6155-6163

Kelly CA, Rudd JWM, St. Louis VL, Heyes A (1995) Is total mercury concentration a good predictor of methyl mercury concentration in aquatic systems? In: Porcella DB, Huckabee JW, Wheatley B (eds) Mercury as a Global Pollutant. Springer, Netherlands, p 715-724

Kelly EN, Short JW, Schindler DW, Hodson PV, Ma M, Kwan AK, Fortin BL (2009) Oil sands development contributes polycyclic aromatic compounds to the Athabasca River and its tributaries. PNAS 106:22346-22351

Kelly EN, Schindler DW, Hodson PV, Short JW, Radmanovich R, Nielson CC (2010) Oil sands development contributes elements toxic at low concentrations to the Athabasca River and its tributaries. PNAS 107:16178-16183

King JK, Kostka JE, Frischer ME, Saunders FM (2000) Sulfate-reducing bacteria methylate mercury at variable rates in pure culture and in marine sediments. Appl Environ Microbiol 66: 2430-2437

King JK, Kostka JE, Frischer ME, Saunders FM, Jahnke RA (2001) A quantitative relationship that demonstrates mercury methylation rates in marine sediments are based on the community composition and activity of sulfate-reducing bacteria. Environ Sci Technol 35:2491-2496

Kirk JL, Muir DCG, Gleason A, Wang X, Lawson G, Frank R, Lehnherr I, Wrona F (2014) Atmospheric Deposition of Mercury and Methylmercury to Landscapes and Waterbodies of the Athabasca Oil Sands Region. Environ Sci Technol 48:7374–7383

Kirk JL, St. Louis VL, Sharp MJ (2006) Rapid reduction and re-emission of mercury deposited into snowpacks during atmospheric mercury depletion events at Churchill, Manitoba, Canada. Environ Sci Technol 40:7590-7596

Korhola A, Rautio M (2001) Cladocera and Other Branchiopod Crustaceans. In: Smol JP, Birks HJB, Last WM (eds) Tracking Environmental Change Using Lake Sediments, vol 4. Kluwer, Dordrecht, pp 5-41

Krachler M, Zheng J, Fisher D, Shotyk W (2009) Global atmospheric As and Bi contamination preserved in 3000 year old Arctic ice. Global Biogeochem Cycles 23. doi:10.1029/2009GB003471

Kuoppamäki K, Setälä H, Rantalainen AL, Kotze DJ (2014) Urban snow indicates pollution originating from road traffic. Environ Pollut 195:56-63

Kurek J, Kirk JL, Muir DCG, Wang X, Evans MS, Smol JP (2013) The legacy of a half century of Athabasca oil sands development recorded by lake ecosystems. PNAS 110:1761-1766

Kurek J, Weeber RC, Smol JP (2011) Environment trumps predation and spatial factors in structuring cladoceran communities from Boreal Shield lakes. Can J Fish Aquat Sci 68:1408-1419

Kurek J, Korosi JB, Jeziorski A, Smol JP (2010) Establishing reliable minimum count sizes for cladoceran subfossils sampled from lake sediments. J Paleolimnol 44:603-612

Landis MS, Pancras JP, Graney JR, Stevens RK, Percy KE, Krupa S (2012) Receptor modeling of epiphytic lichens to elucidate the sources and spatial distribution of inorganic air pollution in the Athabasca oil sands region. In: Percy KE (ed) Alberta Oil Sands: Energy, Industry and the Environment. Elsevier, Kidlington, Oxford, p 427-467

Landers DH et al (2010) The Western Airborne Contaminant Assessment Project (WACAP): An interdisciplinary evaluation of the impacts of airborne contaminants in western US national parks. Environ Sci Technol 44:855-859

Larose C, Dommergue A, De Angelis M, Cossa D, Averty B, Marusczak N, Soumis N, Schneider D, Ferrari C (2010) Springtime changes in snow chemistry lead to new insights into mercury methylation in the Arctic Geochim Cosmochim Acta 74:6263-6275

Lehnherr I, St. Louis VL (2009) Importance of ultraviolet radiation in the photodemethylation of methylmercury in freshwater ecosystems. Environ Sci Technol 43:5692-5698

Lehnherr I, St. Louis VL, Emmerton CA, Barker JD, Kirk JL (2012) Methylmercury cycling in high Arctic wetland ponds: Sources and sinks. Environ Sci Technol 46:10514-10522

Manzano, C, Muir, DCG, Kirk, JL, Teixeira, C, Siu, M, Wang, X, Charland, JP, Schindler, D, Kelly, E. 2016. Temporal variation in the deposition of polycyclic aromatic compounds in snow in the Athabasca Oil Sands area of Alberta. Environmental Monitoring and Assessment 188: 542.

Michelutti N, Blais JM, Cumming BF, Paterson AM, Rühland KM, Wolfe AP, Smol JP (2010) Do spectrally-inferred determinations of chlorophyll a reflect trends in lake trophic status? J Paleolimnol 43(2):205-17

Government of Alberta (2015) MywildAlberta.com-fishconsumptionadvisory. http://mywildalberta.com/Fishing/SafetyProcedures/FishConsumptionAdvisory.aspx. Accessed January 2015.

National Pollutant Release Inventory (NPRI) (2014) http://www.ec.gc.ca/inrp-npri/donnees-data/index.cfm?lang=En. Accessed January 2014.

Laird KR et al (2013) Paleolimnological assessment of limnological change in 10 lakes from northwest Saskatchewan downwind of the Athabasca oils sands based on analysis of siliceous algae and trace metals in sediment cores. Hydrobiologia 720:55-73

Neville LA, Patterson RT, Gammon P, Macumber AL (2013) Relationship between ecological indicators (Arcellacea), total mercury concentrations and grain size in lakes within the Athabasca oil sands region, Alberta. Environ Earth Sci 72:577-588

Parajulee, A, Wania, F (2014) Evaluating officially reported polycyclic aromatic hydrocarbon emissions in the Athabasca oil sands region with a multimedia fate model. PNAS 111:3344–3349

Poulain AJ, Garcia E, Amyot M, Campbell PGC, Raofie F, Ariya A (2007) Biological and chemical redox transformations of mercury in fresh and salt waters of the high Arctic during spring and summer. Environ Sci Technol 41:1883-1888

Pirrone N, Cinnirella S, Feng X, Finkelman RB, Friedli HR, Leaner J, Mason R, Stracher GB, Streets DG, Telmer K (2010) Global mercury emissions to the atmosphere from anthropogenic and natural sources. Atmos Chem Phys 10:5951-5964

Rudd JWM (1995) Sources of methyl mercury to freshwater ecosystems: A review. Water Air Soil Pollut 80:697-713

Rühland KM, Paterson AM, Keller W, Michelutti N, Smol JP (2013) Global warming triggers the loss of a key Arctic refugium. P Roy Soc Lond B Bio 280(1772):20131887. doi:10.1098/rspb.2013.1887

Rühland KM, Paterson AM, Smol JP (2015) Lake diatom responses to warming: reviewing the evidence. J Paleolimnol 54:1-35

Sabag SF (2008) Technical report on the polymetallic black shale SBH Property: Birch Mountains, Athabasca Region, Alberta, Canada. Dumont Nickel Inc, Toronto, Ontario

Savinov, VM, Savinova, TN, Carroll, J et al (2000) Polycyclic aromatic hydrocarbons (PAHs) in sediments of the White Sea, Russia. Mar Pollut Bull 40:807-818

Schroeder WH, Munthe J (1998) Atmospheric mercury-an overview. Atmos Environ 32:809-822

Sellers P, Kelly CA, Rudd JWM (2001) Fluxes of methylmercury to the water column of a drainage lake: the relative importance of internal and external sources. Limnol Oceanogr 46: 632-631

Sharp M, Skidmore M, Nienow P (2002) Seasonal and spatial variations in the chemistry of a high Arctic supraglacial snow cover. J Glaciol 48:149-158

Sherman LS, Blum JD, Johnson KP, Keeler GJ, Barres JA, Douglas TA (2010) Mass-independent fractionation of mercury isotopes in Arctic snow driven by sunlight. Nat Geosci 3:173-177

Shotyk W et al (2014) Sphagnum Mosses from 21 Ombrotrophic Bogs in the Athabasca Bituminous Sands Region Show No Significant Atmospheric Contamination of "Heavy Metals". Environ Sci Tech 48(21):12603-12611

Shotyk W, Krachler M, Martinez-Cortizas A, Cheburkin AK, Emons H (2002) A peat bog record of natural, pre-anthropogenic enrichments of trace elements in atmospheric aerosols since 12 370 14C yr BP, and their variation with Holocene climate change. Earth Planet Sci Lett 199:21-37

Smol JP, Douglas MSV (2007) From controversy to consensus: making the case for recent climate change in the Arctic using lake sediments. Front Ecol Environ 5(9):466-74

St. Louis VL, Rudd JWM, Kelly CA, Beaty KG, Bloom NS, Flett RJ (1994) Importance of wetlands as sources of methyl mercury to boreal forest ecosystems. Can J Fish Aquat Sci 51:1065-1076

Studabaker WB, Krupa S, Jayanty RKM, Raymer JH (2012) Chapter 17 - Measurement of Polynuclear Aromatic Hydrocarbons (PAHs) in Epiphytic Lichens for Receptor Modeling in the Athabasca Oil Sands Region (AOSR): A Pilot Study. Developments in Environmental Science, Vol 11: 391-425

Summers, J, Kurek, J, Kirk, JL, Muir, DCG, Wang, X, Wiklund, JA, Cooke, CA, Evans, MS, Smol, JP (2016) Recent Warming, Rather than Industrial Emissions of Bioavailable Nutrients, is the Dominant Driver of Lake Primary Production Shifts across the Athabasca Oil Sands Region. DOI:10.1371/journal.pone.0153987.

Ullrich SM, Tanton TW, Abdrashitova SA (2001) Mercury in the aquatic environment: A review of factors affecting methylation. Crit Rev Environ Sci Technol 31:241-293

Vallelonga P et al (2002) The lead pollution history of Law Dome, Antarctica, from isotopic measurements on ice cores: 1500 AD to 1989 AD. Earth Planet Sci Lett 204:291-306

Watmough SA, Whitfield CJ, Fenn ME (2014) The importance of atmospheric base cation deposition for preventing soil acidification in the Athabasca Oil Sands Region of Canada. Sci Tot Environ 493:1-11

Weyhenmeyer GA (2001) Warmer winters: Are planktonic algal populations in Sweden's largest lakes affected? Ambio 30(8):565-2

Wiklund JA et al (2014) Use of pre-industrial floodplain lake sediments to establish baseline river metal concentrations downstream of Alberta oil sands: a new approach for detecting pollution of rivers. Environ Res Lett 9:124019. doi:10.1088/1748-9326/9/12/124019

Wiklund JA et al (2012) Has Alberta oil sands development increased far-field delivery of airborne contaminants to the Peace-Athabasca Delta? Sci Tot Environ 433:379-382

Wolfe AP, Vinebrooke RD, Michelutti N, Rivard B, Das B (2006) Experimental calibration of lake-sediment spectral reflectance to chlorophyll a concentrations: Methodology and paleolimnological validation. J Paleolimnol 36(1):91-100

Zhang Y, Shotyk, W, Zaccone, C, Noernberg, T, Pelletier, R, Bicalho, B, Froese||, DG, Davies||, L, Martin, JW (2016) Airborne petcoke dust is a major source of polycyclic aromatic hydrocarbons in the Athabasca Oil Sands region. Environ Sci Technol 50:1711–1720